駒瀬勝啓、竹田誠	麻しん排除を目指した麻しん検査診断体制の問題点	病原微生物検出情報	32、41-42	2011
竹田誠、駒瀬勝啓、森嘉生	世界麻疹排除計画の現状と世界麻疹風疹実験室ネットワークの役割	病原微生物検出情報	32、33-34	2011
駒瀬勝啓	麻疹検査診断法とその問題点	小児科	52(9): 1273-1280	2011
三好正浩, 駒込理佳, 長野秀樹, 高橋健一, 岡野素彦 (他9名)	北海道内の事業所で発生した風疹の集団感染事例	病原微生物検出情報	31(9):5-6	2011
竹田誠、駒瀬勝啓	社会情勢の中で変わりゆく麻疹という感染症	BIO Clinica	26:1198-1202	2011
竹田誠、駒瀬勝啓、森嘉生	世界麻疹排除計画の現状と世界麻疹風疹実験室ネットワークの役割	病原微生物検出情報	32(2):3-4	2011
多屋馨子、佐藤弘、新井智、北本理恵、岡部信彦、森 嘉生、竹田誠	2010年度感染症流行予測調査事業風疹感受性調査担当 2010年度風疹血清疫学調査ならびに予防接種率調査—2010年度感染症流行予測調査中間報告(2010年8月現在速報)	病原微生物検出情報	32(9):14-17	2011
皆川洋子	2012年麻疹排除に向かって—現状と未来—	愛知県小児科医会会報	94:3-11	2011
安井善宏、藤原範子、水谷絵美、安達啓一、伊藤雅、小林慎一、山下照夫、藤浦明、皆川洋子、土屋啓三、柴田陽子、水野周久、土屋啓三、櫛原和貴子、長野友、片岡泉、犬塚君雄	フィリピンからのD9型輸入麻疹および関連症例の発生-愛知県	病原微生物検出情報	32: 45-46	2011
森嘉生、大槻紀之、岡本貴世子、坂田真史、駒瀬勝啓、竹田誠	風疹ウイルスの遺伝子解析	病原微生物検出情報	32(9):11-13	2011
Ito M, Suga T, Akiyoshi K, Nukuzuma S, Kon-no M, Umegaki Y, Kohdera U, Ihara T,	Detection of measles virus RNA by SYBR green real time RT-PCR assay.	Pediatr Intern	52:611-615	2010
Akiyoshi K,Suga S, Nukuzuma S, Kon-no M, Shibata M, Itoh M, Ito Masahiro, Ihara T	Reevaluation of laboratory methods for diagnosis of measles.	Jpn J Infect Dis	63:225-228	2010
Shirogane Y, Takeda M, Tahara M, Ikegame S,	Epithelial- mesenchymal transition abolishes the	J Biol Chem	285:20882- 20890	2010

Nakamura T, Yanagi Y.	susceptibility of polarized epithelial cell lines to measles virus.			
Koga R, Ohno S, Ikegame S, Yanagi Y.	Measles Virus-Induced Immunosuppression in SLAM Knock-In Mice.	J Virol.	84:5360-5367	2010
Sakamoto S, Pongkitwitoon B, Nakamura S, Maenaka K, Tanaka H, Morimoto S.	Efficient silkworm expression of single-chain variable fragment antibody against ginsenoside Re using Bombyx mori nucleopolyhedrovirus bacmid DNA system and its application in enzyme-linked immunosorbent assay for quality control of total ginsenosides.	J Biochem.	148(3):335-340	2010
Kawashima Y, Kuse N, Gatanaga H, Naruto T, Fujiwara M, Dohki S, Akahoshi T, Maenaka K, Goulder P, Oka S, Takiguchi M.	Long-term control of HIV-1 in hemophiliacs carrying slow-progressing allele HLA-B*5101.	J Virol.	84(14):7151-7160	2010
Ayata, M., Takeuchi, K., Takeda, M., Ohgimoto, S., Kato, S., Sharma, LB., Tanaka, M., Kuwamura, M., Ishida, H., Ogura, H.	The F gene of the osaka-2 strain of measles virus derived from a case of subacute sclerosing panencephalitis is a major determinant of neurovirulence.	J Virol.	84(21):11189-11199	2010
長野秀樹, 駒込理佳, 井上真紀、工藤伸一, 岡野素彦	2009 年度の北海道における麻疹 PA 抗体保有状況	道衛研所報	60: 79-80	2010
菊地正幸, 村椿絵美, 扇谷陽子, 伊藤はるみ, 高橋広夫, 三觜雄, 長野秀樹, 駒込理佳, 三好正浩, 岡野素彦	中国からの H1 型麻疹ウイルス輸入症例ー札幌市.	病原微生物検出情報	31 (7): 203	2010
安井善宏、伊藤雅、小林慎一、山下照夫、藤浦明、皆川洋子、柴田陽子、水野周久、土屋啓三、櫛原和貴子、長野友、片岡泉、犬塚君雄	愛知県内で検出された D9 型麻疹ウイルス-輸入例を発端とした感染事例	病原微生物検出情報	31(9): 271-272	2010
庵原俊昭	麻疹	小児科	51:544-545	2010
庵原俊昭	麻疹	小児内科	42:s301-s304	2010
赤地重宏、田沼正路、大	三重県内における麻疹患者の発	病原微生物検	31(9):327	2010

熊和行、堀内功一、田中孝明、一見良司、菅秀、庵原俊昭、駒瀬勝啓	生—帰国者を発端としたD9型麻疹ウイルス検出事例	出情報	-328	
岩田眞美、紺野美貴、椎葉桂子、市川英毅、修理淳、七種美和子、宇宿秀三、池淵守、高野つる代、蔵田英志、多屋馨子、駒瀬勝啓	麻しんか伝染性紅斑か診断に迷った症例	病原微生物検出情報	31(9):265-266	2010
駒瀬勝啓	日本の麻疹・風疹の現状と問題点	総合臨床	59:435-440	2010
染谷健二、駒瀬勝啓、竹田誠	麻疹の検査診断法と全数検査診断に向けた取り組み	小児科	51:1311-1318	2010
染谷健二、駒瀬勝啓、竹田誠	麻疹風疹実験室ネットワーク	臨床検査	54(11):1322-1327	2010
竹田誠、駒瀬勝啓	世界麻疹排除計画と世界麻疹風疹実験室ネットワーク	病原微生物検出情報	31、35-36	2010
田原舞乃、染谷健二、竹田誠	ウイルスのリバースジェネティクス	化学療法の領域	26(7)	2010

研究成果の刊行物・別刷

2013年

JVI
Journals.ASM.org

Functional and Structural Characterization of Neutralizing Epitopes of Measles Virus Hemagglutinin Protein

Maino Tahara,[a] Yuri Ito,[b] Melinda A. Brindley,[c] Xuemin Ma,[a] Jilan He,[a] Songtao Xu,[a] Hideo Fukuhara,[b] Kouji Sakai,[a] Katsuhiro Komase,[a] Paul A. Rota,[d] Richard K. Plemper,[c] Katsumi Maenaka,[b] Makoto Takeda[a]

Department of Virology 3, National Institute of Infectious Diseases, Tokyo, Japan[a]; Laboratory of Biomolecular Science, Faculty of Pharmaceutical Sciences, Hokkaido University, Hokkaido, Japan[b]; Department of Pediatrics, Emory University School of Medicine, Atlanta, Georgia, USA[c]; Measles, Mumps, Rubella and Herpesviruses Laboratory Branch, Division of Viral Diseases, Centers for Disease Control and Prevention, Atlanta, Georgia, USA[d]

Effective vaccination programs have dramatically reduced the number of measles-related deaths globally. Although all the available data suggest that measles eradication is biologically feasible, a structural and biochemical basis for the single serotype nature of measles virus (MV) remains to be provided. The hemagglutinin (H) protein, which binds to two discrete proteinaceous receptors, is the major neutralizing target. Monoclonal antibodies (MAbs) recognizing distinct epitopes on the H protein were characterized using recombinant MVs encoding the H gene from different MV genotypes. The effects of various mutations on neutralization by MAbs and virus fitness were also analyzed, identifying the location of five epitopes on the H protein structure. Our data in the present study demonstrated that the H protein of MV possesses at least two conserved effective neutralizing epitopes. One, which is a previously recognized epitope, is located near the receptor-binding site (RBS), and thus MAbs that recognize this epitope blocked the receptor binding of the H protein, whereas the other epitope is located at the position distant from the RBS. Thus, a MAb that recognizes this epitope did not inhibit the receptor binding of the H protein, rather interfered with the hemagglutinin-fusion (H-F) interaction. This epitope was suggested to play a key role for formation of a higher order of an H-F protein oligomeric structure. Our data also identified one nonconserved effective neutralizing epitope. The epitope has been masked by an *N*-linked sugar modification in some genotype MV strains. These data would contribute to our understanding of the antigenicity of MV and support the global elimination program of measles.

Measles virus (MV) used to be a major cause of death in children. The WHO estimated that ~4% of deaths in children under 5 years of age were caused by measles during the period from 2000 to 2003 (1). However, effective vaccination programs have eliminated measles in the Western Hemisphere, and several other countries are approaching measles elimination (2). In the last decade, the number of measles-related deaths was reduced by more than 90% in all WHO regions, except for Southeast Asia (2). This year, the Measles and Rubella Initiative (http://www.measlesinitiative.org/) developed the Global Measles and Rubella Strategic Plan 2012–2020, which aims to reduce global measles mortality by at least 95% compared with 2000 by the end of 2015 and to achieve measles elimination in at least five WHO regions by the end of 2020. One of the factors favoring measles eradication is the monotypic nature of MV. All the available data suggest that measles eradication is biologically feasible (3, 4). However, a biochemical, molecular, and virological basis for the monotypic nature of MV remains to be provided.

MV is an enveloped virus in the genus *Morbillivirus* of the family *Paramyxoviridae* and possesses two types of glycoprotein spikes, the hemagglutinin (H) and fusion (F) proteins, on the viral envelope. The H protein is responsible for binding to cellular receptors on the target host cells. The signaling lymphocyte activation molecule (SLAM) expressed on immune system cells and nectin4 expressed at adherens junctions in epithelia function as the principal receptors for MV (5–8). Binding of the H protein to a receptor triggers F protein-mediated membrane fusion between the virus envelope and the host cell plasma membrane. Although neutralizing Abs directed against each of the viral envelope glycoproteins are elicited, H protein-specific Abs mainly account for the protection against MV infection (9–11). All measles vaccines consist of live attenuated MV strains isolated about a half a century ago. Currently, 24 genotypes are recognized for MV, and all vaccine strains belong to the same single genotype (genotype A) (12). To date, measles vaccines have been effective, despite differences in the endemic genotypes present in different countries or regions. Consequently, based on these observations, there is no evidence to suggest that MV undergoes a major antigenic drift. Nevertheless, several studies have suggested that currently circulating MV strains show antigenic variations, which could potentially affect the efficacy of vaccination (4, 13–17). Many amino acid residues have been documented to constitute a portion of an epitope. The data show that the H protein has several neutralizing epitopes (NEs), which may locate at the receptor-binding site (RBS) or a region interacting with the F protein. A list of amino acids or regions, which may constitute an epitope, and Abs, which recognize these epitopes, has been provided by Bouche et al. (10). Recently, Hashiguchi et al. determined a crystal structure of the head domain of the H protein in complexes with the V domain of SLAM (18). The head domain of the H protein is formed with six β-sheets arranged in a six-bladed propeller fold (19). SLAM binds to a β-sheet using the side of the propeller fold structure (18). The

Received 4 August 2012 Accepted 22 October 2012
Published ahead of print 31 October 2012
Address correspondence to Maino Tahara, maino@nih.go.jp.
Supplemental material for this article may be found at http://dx.doi.org/10.1128/JVI.02033-12.

doi:10.1128/JVI.02033-12

H protein head forms a homodimer, which is further assembled into a tetrameric structure by forming a dimer of dimers (18). These data allowed us to conduct a fine characterization of epitopes on the H protein. In the present study, we identified the location of several neutralizing epitopes on the MV H protein structure, and characterized these epitopes, providing a molecular basis for the sustainability of the monotypic nature of MV.

MATERIALS AND METHODS

Cells. II-18 (20) and B95a (21) cells were maintained in RPMI medium (Invitrogen) supplemented with 7.5% fetal calf serum (FCS). BHK/T7-9 cells constitutively expressing T7 RNA polymerase (22) were maintained in E-MEM (Invitrogen) supplemented with 10% tryptose phosphate broth and 5% FCS. Vero and Vero/hSLAM cells (Vero cells constitutively expressing human SLAM) (23) were maintained in DMEM (GIBCO) supplemented with 7.5% FCS.

MAbs. Mouse monoclonal antibodies (MAbs) (A2, A26, B5, B12, E39, E81, E103, E128, and E185) were raised against the H protein of the Toyoshima MV strain (genotype A), and some of them were reported previously (24–26). Competitive binding enzyme-linked immunosorbent assays (ELISAs) were performed as reported previously (25). Briefly, peroxidase-conjugated B5, B69, B12, A2, A26, or C149 MAb was mixed with various dilutions of an unlabeled MAb (B5, E81, E128, E185, E39, or E103) and then allowed to react with the MV antigen-coated wells for 2 h. The binding of the peroxidase-conjugated MAb to the MV antigens was detected as described previously (27).

Plasmid construction. All full-length genome plasmids were derived from the p(+)MV323 plasmid encoding the antigenic full-length cDNA of the IC-B strain (genotype D3) (28). The p(+)MV323-Luci plasmid, which has an additional transcriptional unit for the *Renilla* luciferase gene, was reported previously (24). The full-length genome plasmids encoding the H gene of different genotype strains were generated by replacing the H gene region of p(+)MV323-Luci with the corresponding cDNA for the Edmonston-tag [A] (29), MVi/Massachusetts.USA/26.09[B3], MVi/New York.USA/22.09[D4], MVi/Vietnam/29.01[D5], MVi/Okinawa.JPN/37.09[D8], MVi/California.USA/5.9[D9], and MVi/Pennsylvania.USA/20.09[H1] strains. Point mutations, Q391R and Q311R, were introduced into the H gene region of p(+)MV323-Luci by site-directed mutagenesis. Similarly, G211S, E235G, Y252H, L284F, L296F, and G302R mutations were independently introduced into the H gene region of p(+)MV323-Ed/H-Luci (plasmid for the IC/Ed-H-Luci virus) (24).

Viruses. IC323-EGFP, IC323-Luci, IC/EdH-EGFP, IC/EdH-Luci, MV323-EGFP-H-β12(N481Y), MV323-EGFP-H8, -H9, -H10, and -H11 were reported previously (24, 30–32). Other recombinant MVs were generated from the respective full-length genome plasmid as reported previously (33).

Neutralizing assay. A suspension of recombinant MV (2,000 PFU per 75 μl) was incubated with serially diluted MAbs for 30 min at 37°C (the first dilution of each MAb was 1:10, followed by 2-fold dilutions). After incubation with the MAb, the virus solution was inoculated into culture media of confluent monolayers of II-18 (nectin4$^+$) and B95a (SLAM$^+$) cells. For recombinant viruses possessing the genotype A H gene (genotype A viruses; IC/EdH-Luci and IC/EdH-EGFP) and their mutants, CD46-dependent infection was blocked by a MAb against CD46 (clone M75) when the assay was performed with II-18 cells. At 2 days postinfection, the luciferase activity in the cells was measured using a Dual-Glo luciferase assay system (Promega). The neutralizing titer was indicated by the maximum dilution point, exhibiting >50% reduction of luciferase activity. The amount of Ig in each MAb solution (mouse ascites) was analyzed by an ELISA that detects the Fc region of Ig (TaKaRa). The neutralizing titers were normalized by the amount of Ig and are shown in the tables. When enhanced green fluorescent protein (EGFP)-expressing recombinant MVs were used for neutralizing assays, monolayers of II-18 and B95a cells in 24-well cluster plates were incubated with neutralized virus samples for 1 h at 37°C. After a 1-h incubation, 200 μl of RPMI medium supplemented with 7.5% fetal bovine serum (FBS) and 100 μg/ml fusion-blocking peptide (Z-D-Phe-Phe-Gly) (Peptide Institute Inc., Osaka, Japan) was added to each well to block a second round of infection by progeny viruses. At 48 h postinfection, the number of EGFP-expressing cells was counted under a fluorescence microscope. The cell number was expressed in cell infectious units (CIU). The number of CIU for each recombinant MV was also determined in the absence of the Ab and compared with that in the presence of the Ab. The number of CIU for each virus without the Ab was set to 100%.

Ab-selected escape mutants. Recombinant MVs (IC323-EGFP and IC/EdH-EGFP) were incubated with a MAb (B5, E81, or E103) (the Ig concentrations were 0.5 to 1.4 mg/ml) for 30 min at 37°C and then propagated in B95a or II-18 cells in the presence of the MAb. At 2 days postinfection, several syncytia expressing EGFP were independently picked up, suspended in a small volume (100 μl) of culture medium, incubated with the respective MAb for 30 min at 37°C, and then cultured with fresh cells. This cycle was repeated twice, and the H gene nucleotide sequences of the selected mutants were determined as reported previously (33).

Replication kinetics. II-18 cells on 6-well plates were infected with recombinant MVs at a multiplicity of infection (MOI) of 0.01 per cell. After various time intervals, cells were harvested with culture medium and determined for their CIU on Vero/SLAM cells (23).

H and F protein coimmunoprecipitation. Monolayers of Vero cells on 6-well plates were transfected with 3 μg of pCG-EdmHn3xFLAG (Edmonston H protein containing an N-terminal triple Flag tag) (34) and 3 μg of pCG-EdmFc2xHA (Edmonston F protein containing a C-terminal double hemagglutinin [HA] tag) (35) in the presence of 100 μM fusion inhibitory peptide. MV H and F protein coimmunoprecipitation was performed as described previously (36). A mixture of CV1/CV4 MAbs (Millipore) served as a reference (1:1,000). MAbs B5, E81, E103, and E128 were used at a dilution of 1:2,000.

H and H-(473-477A) protein immunoprecipitation. Vero cells on 6-well plates were transfected with 6 μg of pCG-EdmHn3xFLAG or pCG-EdmH473-477An3xFLAG (37). At 36 h posttransfection, the cells were lysed in M2 lysis buffer (50 mM Tris-HCl [pH 7.4], 150 mM NaCl, 1 mM EDTA, 1% Triton X-100, protease inhibitors [Roche], 1 mM phenylmethylsulfonyl fluoride [PMSF]), cleared by centrifugation for 30 min at 20,000 × *g* and 4°C, and incubated with MV H protein ectodomain Abs (CV1/CV4 at 1:1,000 or E128 at 1:2,000). Immunoprecipitation, gel fractionation, and detection of Flag-tagged H protein antigenic material was performed as described previously (34).

Pulse-labeling and immunoprecipitation of MV proteins. At 36 h postinfection, Vero/hSLAM cells infected with recombinant MVs were cultured in methionine-cysteine-deficient medium for 1 h, pulse-labeled with [^{35}S]methionine-cysteine using EasyTag EXPRE35S35S protein labeling mix (PerkinElmer), and then lysed in radioimmunoprecipitation assay (RIPA) buffer. Polypeptides in the cell lysate were immunoprecipitated with a rabbit polyclonal Ab raised against the Toyoshima MV strain and analyzed by SDS-PAGE as reported previously (38). For endoglycosidase H (Endo-H) digestion, immunoprecipitated samples were eluted in 50 mM Tris-HCl (pH 7.4) containing 0.5% SDS by boiling for 4 min. The supernatants were then mixed with 0.1 M sodium citrate buffer (pH 5.3) containing Endo-H and incubated overnight at 37°C.

Surface plasmon resonance assay. Surface plasmon resonance assays were performed using a Biacore 3000 (GE Healthcare) as reported previously (19). Briefly, the biotinylated H protein head domain was immobilized using a biotin capture kit (GE Healthcare) at 400 response units for binding experiments. A solution including each MAb was applied to the chip at a saturated state. Next, soluble human SLAM ectodomain comprising the N-terminal Ig V set domain tandemly connected to the corresponding Ig C2 set domain of mouse SLAM, which largely improves the protein stability, was placed on the chip at a flow rate of 10 ml/min at 25°C. Biotinylated bovine serum albumin (BSA) was used as a negative control. It was difficult to determine the proper regeneration conditions, because the immobilized MV H protein head domain was not as stable under

TABLE 1 Summary of competitive binding ELISAs of anti-H protein MAbs

Unlabeled Ab[a]	Antigenic site	Antigenic site, peroxidase-labeled Ab[b]					
		I, B5[a]	*I*, B69	*I*, B12	*II*, A2	*II*, A26	*III*, C146
B5	*I*	++	++	++	−	+	−
E81	*I*	++	++	++	−	−	−
E128	*II*	−	−	−	++	−	−
E185	*iv*	−	−	−	−	−	+
E39	*v*	−	−	+	−	−	−
E103	*vi*	−	−	−	−	−	−

[a] MAbs used for neutralizing assays in the present study.
[b] ++, complete inhibition; +, partial inhibition; −, no inhibition.

typical regeneration conditions, such as acidic pH, basic pH, or other organic solutions. Therefore, we immobilized the same level of the H protein head domain for each binding experiment.

RESULTS

Antigenic sites *I*, *II*, and *vi* are effective neutralizing epitopes, and all except antigenic site *II* are conserved among different genotypes. In 1985, Sato et al. (25) reported various sets of MAbs against MV structural proteins. In the study, 11 MAbs recognizing the H protein were characterized in detail. Based on competitive ELISA data, three nonoverlapping or partially overlapping antigenic sites (*I*, *II*, and *III*) in the H protein were predicted (25). In addition to these 11 MAbs, we analyzed a further five MAbs (E81, E128, E185, E39, and E103) directed against the H protein by competitive binding ELISAs (Table 1). E81 and E128 completely inhibited the binding of MAbs recognizing antigenic sites *I* and *II*, respectively (Table 1). On the other hand, neither E185, E39, nor E103 showed complete inhibition against the binding of MAbs recognizing antigenic sites *I*, *II*, and *III*. E39 and E185 only partially inhibited the binding of MAbs recognizing antigenic sites *I* and *III*, respectively (Table 1). E103 showed no competitive inhibition against the binding of MAbs recognizing antigenic sites *I*, *II*, and *III*. Based on these data, we tentatively predicted antigenic sites *iv*, *v*, and *vi*, which were recognized by E185, E39, and E103, respectively (Table 1). The newly tested MAbs (E81, E128, E185, E39, and E103) and B5 reported by Sato et al. (25) were then used for MV neutralizing assays. The antigenic site recognized by each MAb is shown in parentheses: B5(*I*), E81(*I*), E128(*II*), E185(*iv*), E39(*v*), and E103(*vi*). Eight distinct recombinant MVs were used as neutralization targets (Table 2; see also Table S1 in the supplemental material). These recombinant MVs were based on the IC323 genomic background and encoded a *Renilla* luciferase reporter gene and an H gene derived from different MV genotypes (A, B3, D3, D4, D5, D8, D9, and H1) (see Table S1) (28, 39). They were named on the basis of the genotype of the H gene: genotype A, B3, D3, D4, D5, D8, D9, and H1 viruses. MAbs B5(*I*), E81(*I*), E128(*II*), and E103(*vi*) showed high neutralizing titers in SLAM$^+$ B95a and/or nectin4$^+$ II-18 cells (20, 21). While B5(*I*), E81(*I*), and E103(*vi*) neutralized all of the MV genotypes tested, E128(*II*) was only effective against genotype A, B3, D8, and H1 viruses (Table 2). The neutralizing titers of E185(*iv*) and E39(*v*) were significantly lower than those of B5(*I*), E81(*I*), E128(*II*), and E103(*vi*) (Table 2). These data suggest that antigenic sites *I*, *II*, and *vi* are effective neutralizing epitopes and that, with the exception of antigenic site *II*, all epitopes are conserved among the different MV genotypes.

Antigenic site *I* is located near the RBS, while antigenic site *vi* is located at a position distant from the RBS. To identify the locations of antigenic sites on the H protein, EGFP-expressing

TABLE 2 Neutralizing titers against MV strains possessing H genes from different genotypes

Cell line	Genotype, year isolated	Neutralizing titer against recombinant MV strain[a]:					
		B5(*I*)	E81(*I*)	E128(*II*)	E185(*iv*)	E39(*v*)	E103(*vi*)
B95a	A, 1954	30,144	863	1,968	494	<27	2,558
	B3, 2009	60,288	1,727	1,968	987	<27	10,231
	D3, 1984	7,536	1,727	15	31	<27	10,231
	D4, 2009	30,144	1,727	31	62	<27	20,462
	D5, 2001	30,144	863	15	494	<27	10,231
	D8, 2009	60,288	1,727	1,968	987	<27	20,462
	D9, 2010	60,288	1,727	15	987	<27	20,462
	H1, 2009	30,144	1,727	1,968	494	<27	20,462
II-18	A, 1954	30,144	27,631	62,977	124	1,750	10,231
	B3, 2009	30,144	27,631	62,977	1,974	1,750	10,231
	D3, 1984	3,768	27,631	123	62	<27	20,462
	D4, 2009	30,144	27,631	31	<8	<27	10,231
	D5, 2001	30,144	27,631	<4	1,974	<27	20,462
	D8, 2009	60,288	27,631	62,977	987	<27	10,231
	D9, 2010	60,288	27,631	123	1,974	<27	10,231
	H1, 2009	15,072	13,815	62,977	494	1,750	10,231

[a] Neutralizing titers for 1 mg/ml of Ig.

TABLE 3 Neutralizing titers against recombinant MVs possessing the H protein of genotye D3 virus with amino acid substitutions

Cell line	Mutation	Neutralizing titer against recombinant MV[a]: B5(*I*)	E81(*I*)	E103(*vi*)
B95a	wt: (−)	7,536	1,727	10,231
	Q391R	<471	<14	20,462
	Q311R	1,884	1,727	80
II-18	wt: (−)	3,764	27,631	20,462
	Q391R	<4	<3	20,462
	Q311R	1,884	27,631	20

[a] Neutralizing titers for 1 mg/ml of Ig.

MVs (IC323-EGFP) (30) that escaped from neutralization were isolated, and the amino acid changes in the H protein were identified by sequence analysis. Of the two escape mutants obtained, one escaped from neutralization by E81(*I*) through a Q391R mutation, and the other escaped E103(*vi*) through a Q311R mutation. These mutations were rebuilt in the luciferase gene-encoding recombinant IC323-Luci genome (24) by site-directed mutagenesis and reverse genetics (see Table S1 in the supplemental material). The resulting IC323-Luci-H(Q391R) was largely resistant to B5(*I*) but neutralized by E103(*vi*) with similar efficiency to that found for the parental virus (Table 3). The IC323-Luci-H(Q311R) recombinant was neutralized efficiently by B5(*I*) and E81(*I*) but escaped from neutralization by E103(*vi*) (Table 3). The amino acid residues at positions 391 and 311 are located within previously recognized epitopes on the H protein (10, 18, 19), which apparently correspond to antigenic sites *I* and *vi* (Fig. 1B and Table 4). The amino acid changes observed in the escape mutants indicate that antigenic site *I* is located near the SLAM-binding site, while antigenic site *vi* is located at a more distal position, although both act as effective neutralizing epitopes (Fig. 1B and Table 2). Mutagenesis of the H protein confirmed that the nectin4-binding site is distinct from the SLAM-binding site but probably shows a partial overlap (32, 40). This is consistent with the neutralization of MV by B5(*I*) and E81(*I*) on II-18 cells (Table 2). Epitope *vi* recognized by E103 corresponds to the previously predicted epitope recognized by BH38 and I-29 (Table 4) (10, 41, 42). Importantly, H mutants with Q391R or Q311R replicated somewhat less efficiently than the parental virus in cultured cells (Fig. 2), suggesting conformational effects of these changes on the H protein structure.

Antigenic site *II* is located near the bottom surface of the H protein head domain and is shielded by *N*-glycans attached to residue 416 in recent outbreak strains of MV. As described above, E128(*II*) neutralized several MV genotypes but failed to neutralize genotype D3, D4, D5, and D9 viruses (Table 2). Comparison of the H protein sequences of various MV genotypes indicated that the H proteins of MV genotypes D3, D4, D5, and D9, but not of genotypes A, B2, D8, and H1, harbor an additional potential site for *N*-linked glycosylation at residue 416 (see Fig. S1 in the supplemental material) (17, 43, 44). The electrophoretic mobility of the H proteins of genotype D3, D4, D5, and D9 was markedly reduced compared with that of the H proteins of genotypes A, B3, D8, and H1 (Fig. 3A), suggesting that an additional *N*-glycan moiety may be present on the H proteins of the former genotypes. Follow-up analyses with recombinant MV variants featuring a chimeric H gene combining fragments of the IC323 (genotype D3) and Edmonston (genotype A) strains (see Table S1) (31) showed that the amino acid difference at position 416 served as a determinant for the differential response to neutralization by E128(*II*) (Fig. 2B and C and Table 5). The addition of an *N*-glycan was confirmed by endoglycosidase H (Endo-H) treatment (Fig. 3D) as reported previously (17). In addition, the H protein of the Edmonston strain entirely lost its reactivity with E128(*II*) when carrying amino acid substitutions at positions 473 to 477 (Fig. 3E) (34). The epitope *II* likely constitutes a portion of RBS, since the amino acid region at positions 473 to 477 is involved in interaction with CD46, a receptor for MV vaccine strains (10, 45). Taken together, these data underscore that the *N*-glycan at position 416 masked epitope *II*, one of the major antigenic sites, which is located in the vicinity of a CD46-binding site (Fig. 1C). However, it was previously reported that serum samples derived

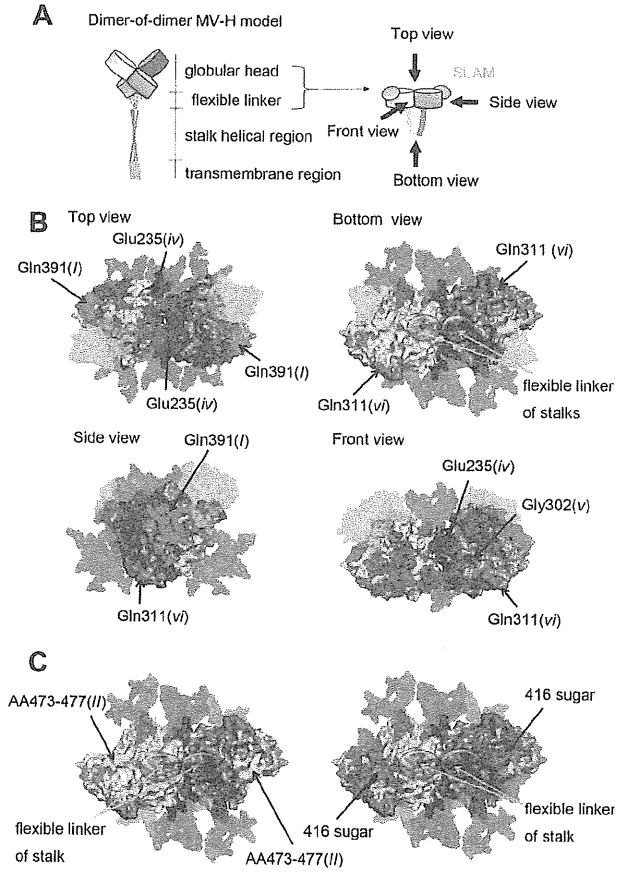

FIG 1 Locations of epitopes on the H protein dimeric structure. (A) Diagrams of a dimer of H protein dimers. The four H protein molecules are shown in gray, light gray, purple, and light purple. SLAM is shown in cyan. (B) Locations of epitopes *I*, *iv*, and *vi*. SLAM and predicted *N*-linked sugars are shown in translucent cyan and magenta, respectively. The amino acid residues demonstrated or suggested to constitute a portion of an epitope are shown in colors: residues on β-sheets 1, 2, 3, 4, 5, and 6 (18) are shown in blue, green, light green, yellow, orange, and red, respectively. (C) Location of epitope *II*. H protein dimers without (left) and with (right) the *N*-linked sugar at position 416 are shown. The figures were produced using PyMOL (Schrödinger; http://www.pymol.org).

TABLE 4 Relation between epitopes and Abs[a]

Epitope name		Region or amino acids which constitute an epitope	Ab which recognizes the epitope	
Present study	Previous papers		Present study	Previous papers
		126–135		MAb48
		185–195		I-44
iv		233–240	E185	BH1
	NE	244–250		BH47, BH59, BH129
v		302	E39	
vi		309–318	E103	I-29, BH38
I	HNE	380–400	E81, B5	BH6, BH21, BH216
		377		BH171
		378		BH168
II		473–477	E128	
		491		16-CD-11
		505–506		80-II-B2
		552		I-41
		587–596		MAb18

[a] Relation between epitopes and Abs in the present and previous studies (10, 41, 42, 47, 51, 53).

from vaccine recipients neutralized all MV strains efficiently, regardless of the glycosylation status at residue 416 (17). Thus, this glycosylation site does not amount to a serious concern with regard to current MV vaccines. However, the additional carbohydrate moiety may provide some advantage for the endemic spread of MV, since the MV strains associated with recent large outbreaks in Europe and Southeast Asia (D4 and D9, respectively) possess this glycosylation site (see Fig. S1 and S2 in the supplemental material) (46). On the other hand, the genotype H1 and D8 strains, which are currently endemic in China and India, respectively, do not have this extra glycosylation site (see Fig. S1 and S2).

Antigenic sites *iv* and *v*, located at the lateral surface of the H protein head dimer, are less important for neutralization. In contrast to genotype D3, MV strains of genotype A were neutralized by E185(*iv*) and E39(*v*) in SLAM$^+$ B95a cells and nectin4$^+$ II-18 cells, respectively (Table 2). We further tested two recombinant MVs possessing chimeric H genes derived from genotypes A and D3 or featuring point mutations [MV323-EGFP-H-β12(N481Y) and MV323-EGFP-H8] (31) for neutralization by E185(*iv*) and E39(*v*) (Fig. 4 and Table 5; see also Table S1 in the supplemental material). The neutralization data demonstrated that amino acids within residues 174 to 334 determined the difference in neutralization by E185(*iv*) and E39(*v*) between MVs with genotypes A and D3. Amino acid substitutions present in this region and predicted to be exposed on the H protein surface (19) were individually introduced into a genotype A virus, resulting in the generation of six additional MVs (Table 6; see also Table S1 in the supplemental material). These recombinant MVs were subjected to neutralization analyses. H protein mutations E235G and G302R rendered the recombinant MVs resistant to neutralization by E185(*iv*) and E39(*v*), respectively (Table 6). These data suggested that residues 235 and 302 are part of epitopes *iv* and *v*, respectively. Epitope *iv* is therefore likely to correspond to the previously reported epitope recognized by BH1 (amino acids 233 to 240 are critical for BH1 binding) (Fig. 5 and Table 4) (47). Both residues are located at the lateral surface of the H protein head dimer, distal from the RBS (Fig. 1B). Furthermore, these epitopes are quite close to the *N*-linked sugars, which may exert some steric hindrance to reduce the binding activities of the Abs (Fig. 1B). These observations are consistent with the weak neutralizing phenotypes of E185(*iv*) and E39(*v*) (Table 2).

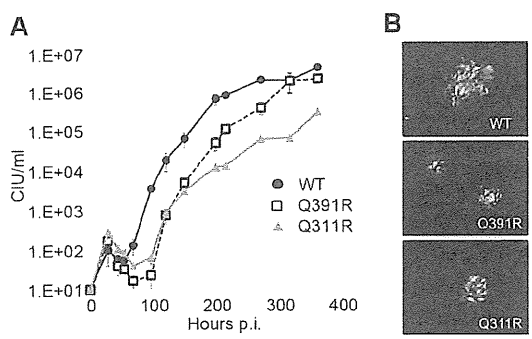

FIG 2 Replication kinetics of two recombinant MVs possessing Q311R or Q391R mutations. (A) Replication kinetics of two escape mutants in II-18 cells. II-18 cells were infected with the MVs at an MOI of 0.01. At various time intervals, cells were harvested in the culture medium and their CIU values were determined in Vero/hSLAM cells. (B) EGFP autofluorescence in MV-infected monolayers of II-18 cells. Panels show representative images obtained with a fluorescence microscope at 6 days postinfection.

Neutralizing Abs that recognize antigenic sites *I* and *II* inhibit receptor binding, while neutralizing Abs specific for antigenic site *vi* interfere with the H-F protein interaction. To mechanistically explore the basis for neutralization by the different MAbs, the effects of the MAbs on the interaction between the H protein (genotype A) and SLAM were analyzed by binding assays using surface plasmon resonance (Biacore assays). MAbs B5(*I*), E81(*I*), and E128(*II*) blocked the binding of the H protein to SLAM, whereas E103(*vi*) did not (Table 7), although all of the MAbs had high neutralization activities (Table 2). These data are consistent with the observations that epitopes *I* and *II* are located near the RBS (10, 45), while epitope *vi* has a more distal position (Fig. 1B). It remains uncertain how epitope *vi* can be a major neutralizing target site. It can be speculated that the epitope may

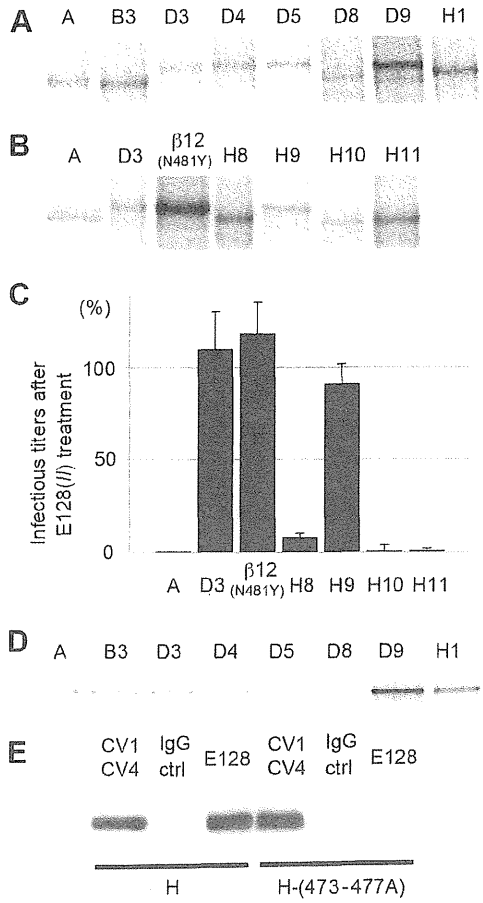

FIG 3 Masking of epitope *II* by the N416-linked sugar. (A) SDS-PAGE analyses for the mobility of H proteins of different genotypes. MV-infected Vero/hSLAM cells at 36 h postinfection were labeled with [^{35}S]methionine-cysteine and lysed in RIPA buffer. Polypeptides were then immunoprecipitated with a polyclonal Ab against MV and resolved by SDS-PAGE. (B) SDS-PAGE analyses for the mobility of H proteins of previously reported recombinant MVs possessing a chimeric H gene between the IC323 (genotype D3) and Edmonston (genotype A) strains or various point mutations. (C) Neutralizing assays of E128 against EGFP-expressing MV strains possessing a chimeric H gene between the IC323 (genotype D3) and Edmonston (genotype A) strains or various point mutations. The CIU of each virus was determined in II-18 cells in the presence or absence of E128. The CIU determined in the presence of E128 was compared with that in the absence of E128. The CIU in the absence of E128 was set to 100%. (D) SDS-PAGE analyses for the mobility of Endo-H-treated H proteins of different genotypes. (E) A five-residue alanine substitution in the H protein at residues 473 to 477 prevents binding of MAb E128. Immunoprecipitation of MV H_{Flag} and CD46-binding defective MV H_{Flag}-(473-477A) with MAbs CV1/CV4 and E128. The immunoprecipitated material was gel fractionated, followed by immunoblotting and detection of H_{Flag} with an anti-Flag M2 antibody. IgG ctrl; control IgG.

TABLE 5 Amino acid differences in recombinant MVs

Amino acid position	Amino acid difference in recombinant MV[a]:						
	A	D3	β12(N481Y)	H8	H9	H10	H11
174	T	A	T	A	A	A	A
176	T	A	T	A	A	A	A
211	G	S	G	S	S	S	S
235	E	G	E	G	G	G	G
243	K	G	K	G	G	G	G
252	Y	H	Y	H	H	H	H
276	L	F	L	F	F	F	F
284	L	F	L	F	F	F	F
296	L	F	L	F	F	F	F
302	G	R	G	R	R	R	R
334	Q	R	Q	R	R	R	R
390	I	N	N	I	I	N	I
416	D	N	N	D	N	D	D
446	S	T	T	T	S	S	S
481	Y	N	Y	Y	Y	Y	Y
492	G	E	E	G	G	G	E
575	Q	K	K	K	K	K	K

[a] These recombinant MVs were reported previously (31).

be involved in one or some of the fusion steps other than the receptor binding. To examine whether the H-F protein interaction affects MAb binding, coimmunoprecipitation of MV envelope glycoprotein complexes was performed (36). Compared with a reference Ab cocktail, the amount of F protein coimmunoprecipitated with H protein was reduced by ~50% when E103(*vi*) was used (Fig. 6). These data suggested that epitope *vi* is influenced by the H-F protein interaction. Interestingly, the higher order (tetrameric) structures of the H protein-SLAM complex proposed on the basis of the crystal structures suggest that epitope *vi* in two of the four H molecules (gray and light purple H molecules) is located at the bottom surface proximal to the stalk region, while that in the other two molecules (light gray and purple H molecules) forms part of the interface of the H protein dimers in form I, one of the tetrameric structures (Fig. 7A) (18), but not form II, the other tetrameric structure (Fig. 7B) (18). Furthermore, epitope *vi* appears to contact epitope *iv* at the interface (Fig. 7A). Epitope *iv* corresponds to the BH1-binding epitope (Table 4) (47), and most likely forms a single epitope together with a previously reported linear neutralizing epitope (NE) (amino acid positions 244 to 250) (Table 4) (47), although a definitive conclusion could not be made, because eight amino acids (positions 240 to 247) were so flexible that little electron density was observed in the H crystal structures (Fig. 5) (18).

DISCUSSION

In the present study, we focused on neutralizing Abs directed against the H protein, because the protective immunity is predominantly humoral (48) and H protein-specific Abs mainly account for the neutralization activity in serum from vaccinated

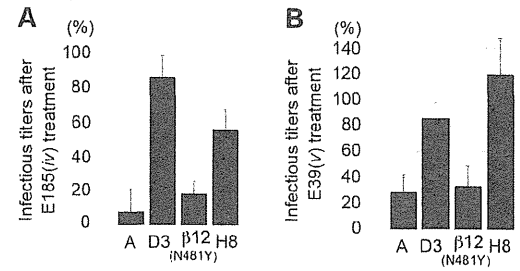

FIG 4 Neutralizing assays of E185 and E39 against EGFP-expressing MV strains with different H protein sequences. (A) The CIU of each virus was determined in B95a cells in the presence or absence of E185. (B) The CIU of each virus was determined in II-18 cells in the presence or absence of E39. The CIU determined in the presence of the Abs was compared with that in the absence of the Abs. The CIU in the absence of the Abs was set to 100%.

TABLE 6 Neutralizing titers against recombinant MV possessing the Edmonston H protein with various amino acid substitutions[a]

Mutation	Neutralizing titer against recombinant MV:	
	E185(*iv*) in B95a	E39(*v*) in II-18
(−)	494	1,750
G211S	494	875
E235G	62	1,750
Y252H	494	1,750
L284F	494	1,750
L296F	494	1,750
G302R	494	<27

[a] Neutralizing titers for 1 mg/ml of Ig. (−), parental virus.

TABLE 7 Competitive binding of anti-H protein MAbs against SLAM

Ab	Antigenic site	Competitive activity[a]
B5	*I*	++
E81	*I*	+
E128	*II*	++
E103	*vi*	−

[a] ++, Complete inhibition; +, weak inhibition; −, no inhibition.

individuals (9–11). A key finding in the present study is that the antigenic site *vi*, which is unrelated to receptor binding but probably involved in the formation of a higher-order H-F protein oligomeric structure (34, 36, 49), is a major neutralizing epitope that is conserved among different genotype strains. This type of epitopes has been predicted by previous studies, although receptor binding has been tested for CD46, but not the wild-type receptors, SLAM, or nectin4 (10, 47, 50). One of them, known as NE, is recognized by BH47, BH59, and BH129 MAbs (Table 4) (10, 47). The other is recognized by I-29 (10, 50) and was determined as the epitope *vi* in the present study (Table 4). Therefore, our data are consistent with the previous studies that MAbs that recognize the epitope *vi* neutralize MV infection by inhibiting virus fusion without affecting the receptor binding (10, 50). Membrane fusion of MV is mediated by concerted actions of the H and F proteins. Binding of the H protein to a receptor triggers F protein-mediated membrane fusion. Although the triggering mechanism remains largely unknown, accumulated data indicate that rearrangement of an H-F protein oligomeric structure is a key for triggering fusion (18, 34, 36, 49). This epitope is fully conserved among different MV genotypes. A requirement for the formation of a functional fusion complex is likely to generate structural constraints that prevent substitutions in this epitope.

We also found that a large area containing epitopes *I* and *II* serves as a target for the humoral anti-MV response. Our data showed that MAbs B5 and E81 bind to an epitope (epitope *I*) corresponding to a previously reported hemagglutination and neutralization epitope (HNE) (amino acid positions 380 to 400), which is recognized by MAbs BH6, BH21, and BH216 (Table 4 and Fig. 8) (10, 41, 51). Six residues (positions 386, 387, 388, 391, 394, and 395) were shown to be critical for Ab binding (52). Accordingly, a Q391R substitution was sufficient for MV escape from neutralization by B5 and E81. On the other hand, epitope *II* maps to residues 473 to 477, which are located at the bottom surface of the H protein head domain and involved in interaction with CD46 (10, 45). In some of the current wild-type MV strains,

TYLVEKPNLSSKRSELSQLSMY
AA233-240: BH1-binding site AA244-250: NE

TYLVEKPNL--------QLSMY

FIG 5 Amino acid sequence of epitope *iv*. The amino acid residues at positions 231 to 252 are shown. The residues known to constitute part of the epitope are shown in blue characters (top). The amino acid residues represented in the crystal structures are shown. Missing residues are indicated by dashes.

this epitope is masked by an additional carbohydrate moiety (Asn416). Previous studies revealed that MV escape from MAb 16-CD-11 can be achieved through an amino acid substitution at position 491 in the H protein (41) and that escape mutants from MAbs BH171 and BH168 possess substitutions at positions 377 and 378, respectively (Table 4) (10, 53). The residues at positions 491, 377, and 378 in the H protein are located between the HNE (epitope *I*) and epitope *II* (Table 4 and Fig. 8). It was further shown that H protein binding of MAbs BH30 and BH99 competes with 16-CD-11 (10, 41). Taken together, these data support that a large area of the H protein head domain spanning from epitope *I* to epitope *II* can serve as a target for neutralizing Abs (Fig. 8). Our data suggest that the region around epitope *I* has structural con-

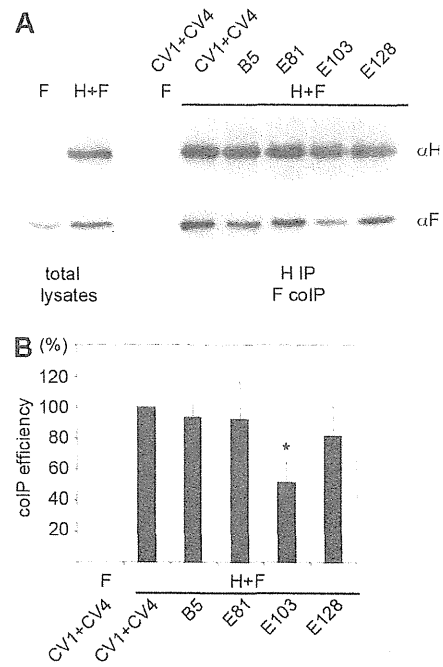

FIG 6 MV H and F protein coimmunoprecipitation. MAb E103 shows reduced immunoprecipitation efficiency for H/F hetero-oligomers. (A) Vero cells transiently transfected with expression plasmids encoding MV H_{Flag} and F_{HA}, or F_{HA} only as a control, were immunoprecipitated with specific MAbs directed against the MV H protein ectodomain (CV1/CV4, B5, E81, E103, or E128 as indicated). Precipitated H_{Flag} material was labeled with an anti-Flag M2 antibody, and the coprecipitated F_{HA} was detected with an anti-HA 16b12 antibody. (B) For densitometric quantification, the ratio of F_{HA} to H_{Flag} signals was determined for each MAb, followed by normalization to the coimmunoprecipitation ratio obtained with the CV1/CV4 reference MAb mixture. Data represent the means ± standard errors of the means (SEM) of results from three experiments. The asterisk indicates that, in F densitometry, a *t* test returned *P* values of <0.05 for the difference in coimmunoprecipitation (CoIP) efficiency, with E103 relative to the CV1+CV4 reference.

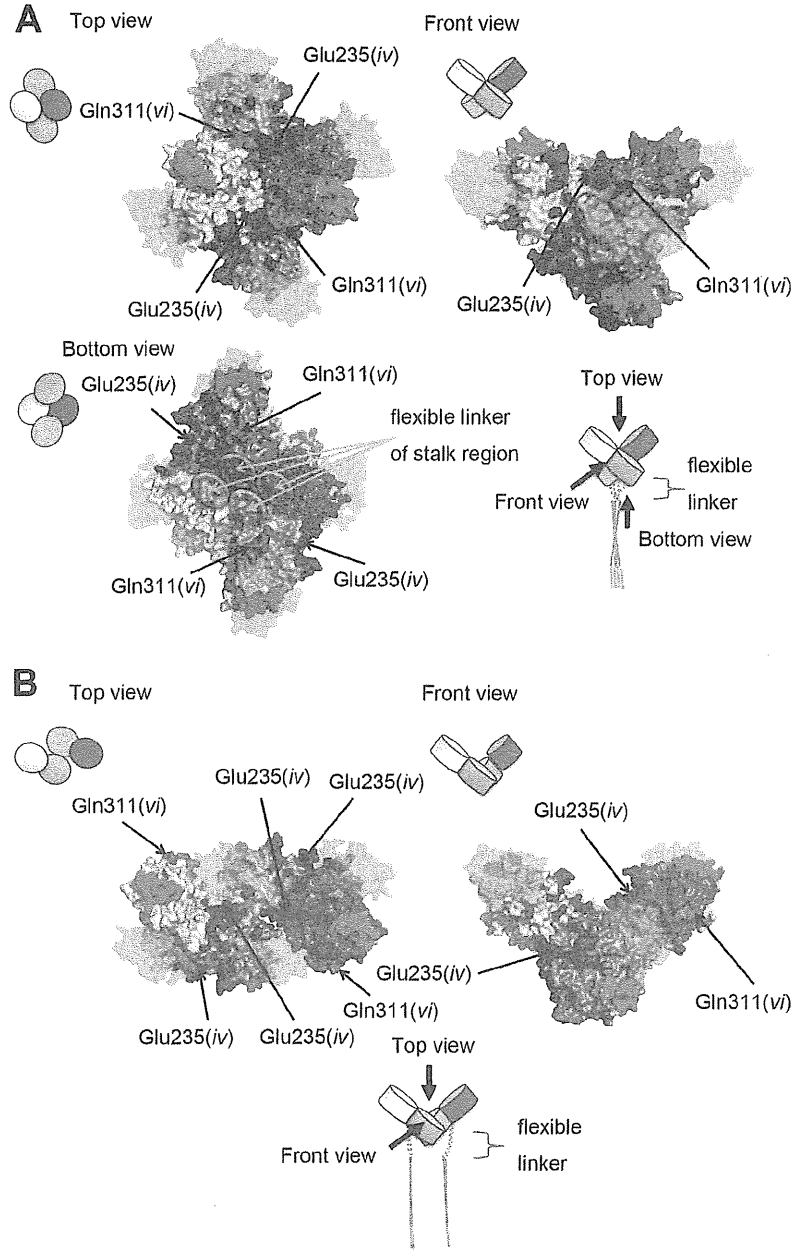

FIG 7 Locations of epitopes *iv* and *vi* on the H protein tetrameric structure. The four H protein molecules are shown in gray, light gray, purple, and light purple. SLAM is shown in translucent cyan. The amino acid residues demonstrated or suggested to constitute a portion of an epitope are shown in colors: residues on β-sheets 1, 2, 3, 4, 5, and 6 (18) are shown in blue, green, light green, yellow, orange, and red, respectively. (A) A tetrameric structure in form I (18). (B) A tetrameric structure in form II (18).

straints for change, since it is conserved among different genotype strains, thereby contributing to the single serotype nature of MV.

In summary, the H protein of MV possesses at least two conserved effective neutralizing epitopes. One, which is a previously recognized HNE epitope, is located near the RBS, and thus MAbs that recognize this epitope blocked the receptor binding of the H protein. On the other hand, the other epitope is located at the position distant from the RBS. Thus, MAbs that recognizes this epitope did not inhibit the receptor binding of the H protein but rather interfered with the H-F interaction. Based on the structural data of MV H protein, it was predicted that, when the H protein forms a tetramer, this epitope locates at two positions: the contact face of two H protein dimers and the bottom face of the head of the H protein tetramer. This epitope possibly plays a key role in the formation of a higher-order H-F protein oligomeric structure. Our data also demonstrated that one effective neutralizing epitope is not conserved, since the epitope has been masked by an *N*-linked sugar modification in some genotype MV strains. The data in the

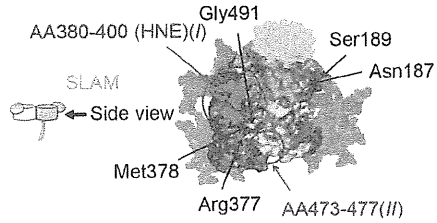

FIG 8 A major epitope region covering a large area containing epitopes *I* and *II*. A side view of a dimer is shown. SLAM and predicted sugars are shown in translucent cyan and magenta, respectively. The amino acid residues demonstrated or suggested to constitute a portion of an epitope are shown in colors: residues on β-sheet 1, 2, 3, 4, 5, and 6 (18) are shown in blue, green, light green, yellow, orange, and red, respectively.

present study contribute to our understanding of the antigenicity of MV and support the global elimination program of measles.

ACKNOWLEDGMENTS

We thank T.A. Sato and T. Seya for providing MAbs, N. Ito and M. Sugiyama for providing the BHK/T7-9 cells, and K. Taira for providing an MV isolate. We also thank Y. Yanagi for invaluable suggestions and providing useful cell lines and all the members of the Department of Virology 3, NIID, Japan, for technical support.

This work was supported in part by grants from the Ministry of Education, Culture, Sports, Science and Technology and the Ministry of Health, Labor and Welfare of Japan and by a grant from The Takeda Science Foundation (to M.T.). The work of M.A.B. and R.K.P. was supported in part by Public Health Service grant AI083402 from the NIH/NIAID (to R.K.P.).

REFERENCES

1. Bryce J, Boschi-Pinto C, Shibuya K, Black RE. 2005. WHO estimates of the causes of death in children. Lancet 365:1147–1152.
2. Strebel PM, Cochi SL, Hoekstra E, Rota PA, Featherstone D, Bellini WJ, Katz SL. 2011. A world without measles. J. Infect. Dis. 204(Suppl 1):S1–S3.
3. Sanders R, Dabbagh A, Featherstone D. 2011. Risk analysis for measles reintroduction after global certification of eradication. J. Infect. Dis. 204(Suppl 1):S71–S77.
4. Bellini WJ, a Rota PA. 2011. Biological feasibility of measles eradication. Virus Res. 162:72–79.
5. Tatsuo H, Ono N, Tanaka K, Yanagi Y. 2000. SLAM (CDw150) is a cellular receptor for measles virus. Nature 406:893–897.
6. Noyce RS, Bondre DG, Ha MN, Lin LT, Sisson G, Tsao MS, Richardson CD. 2011. Tumor cell marker PVRL4 (nectin 4) is an epithelial cell receptor for measles virus. PLoS Pathog. 7:e1002240. doi:10.1371/journal.ppat.1002240.
7. Muhlebach MD, Mateo M, Sinn PL, Prufer S, Uhlig KM, Leonard VH, Navaratnarajah CK, Frenzke M, Wong XX, Sawatsky B, Ramachandran S, McCray PB, Jr, Cichutek K, von Messling V, Lopez M, Cattaneo R. 2011. Adherens junction protein nectin-4 is the epithelial receptor for measles virus. Nature 480:530–533.
8. Takeda M, Tahara M, Nagata N, Seki F. 2011. Wild-type measles virus is intrinsically dual-tropic. Front. Microbiol. 2:279.
9. de Swart RL, Yuksel S, Osterhaus AD. 2005. Relative contributions of measles virus hemagglutinin- and fusion protein-specific serum antibodies to virus neutralization. J. Virol. 79:11547–11551.
10. Bouche FB, Ertl OT, Muller CP. 2002. Neutralizing B cell response in measles. Viral Immunol. 15:451–471.
11. de Swart RL, Yuksel S, Langerijs CN, Muller CP, Osterhaus AD. 2009. Depletion of measles virus glycoprotein-specific antibodies from human sera reveals genotype-specific neutralizing antibodies. J. Gen. Virol. 90:2982–2989.
12. WHO. 2012. Measles virus nomenclature update: 2012. Wkly. Epidemiol. Rec. 87:73–81.
13. Finsterbusch T, Wolbert A, Deitemeier I, Meyer K, Mosquera MM, Mankertz A, Santibanez S. 2009. Measles viruses of genotype H1 evade recognition by vaccine-induced neutralizing antibodies targeting the linear haemagglutinin noose epitope. J. Gen. Virol. 90:2739–2745.
14. Shi J, Zheng J, Huang H, Hu Y, Bian J, Xu D, Li F. 2011. Measles incidence rate and a phylogenetic study of contemporary genotype H1 measles strains in China: is an improved measles vaccine needed? Virus Genes 43:319–326.
15. Tamin A, Rota PA, Wang ZD, Heath JL, Anderson LJ, Bellini WJ. 1994. Antigenic analysis of current wild type and vaccine strains of measles virus. J. Infect. Dis. 170:795–801.
16. Kuhne M, Brown DW, Jin L. 2006. Genetic variability of measles virus in acute and persistent infections. Infect. Genet. Evol. 6:269–276.
17. Santibanez S, Niewiesk S, Heider A, Schneider-Schaulies J, Berbers GA, Zimmermann A, Halenius A, Wolbert A, Deitemeier I, Tischer A, Hebgek H. 2005. Probing neutralizing-antibody responses against emerging measles viruses (MVs): immune selection of MV by H protein-specific antibodies? J. Gen. Virol. 86:365–374.
18. Hashiguchi T, Ose T, Kubota M, Maita N, Kamishikiryo J, Maenaka K, Yanagi Y. 2011. Structure of the measles virus hemagglutinin bound to its cellular receptor SLAM. Nat. Struct. Mol. Biol. 18:135–141.
19. Hashiguchi T, Kajikawa M, Maita N, Takeda M, Kuroki K, Sasaki K, Kohda D, Yanagi Y, Maenaka K. 2007. Crystal structure of measles virus hemagglutinin provides insight into effective vaccines. Proc. Natl. Acad. Sci. U. S. A. 104:19535–19540.
20. Shirogane Y, Takeda M, Tahara M, Ikegame S, Nakamura T, Yanagi Y. 2010. Epithelial-mesenchymal transition abolishes the susceptibility of polarized epithelial cell lines to measles virus. J. Biol. Chem. 285:20882–20890.
21. Kobune F, Sakata H, Sugiura A. 1990. Marmoset lymphoblastoid cells as a sensitive host for isolation of measles virus. J. Virol. 64:700–705.
22. Ito N, Takayama-Ito M, Yamada K, Hosokawa J, Sugiyama M, Minamoto N. 2003. Improved recovery of rabies virus from cloned cDNA using a vaccinia virus-free reverse genetics system. Microbiol. Immunol. 47:613–617.
23. Ono N, Tatsuo H, Hidaka Y, Aoki T, Minagawa H, Yanagi Y. 2001. Measles viruses on throat swabs from measles patients use signaling lymphocytic activation molecule (CDw150) but not CD46 as a cellular receptor. J. Virol. 75:4399–4401.
24. Takeda M, Tahara M, Hashiguchi T, Sato TA, Jinnouchi F, Ueki S, Ohno S, Yanagi Y. 2007. A human lung carcinoma cell line supports efficient measles virus growth and syncytium formation via a SLAM- and CD46-independent mechanism. J. Virol. 81:12091–12096.
25. Sato TA, Fukuda A, Sugiura A. 1985. Characterization of major structural proteins of measles virus with monoclonal antibodies. J. Gen. Virol. 66(Pt 7):1397–1409.
26. Sato TA, Enami M, Kohama T. 1995. Isolation of the measles virus hemagglutinin protein in a soluble form by protease digestion. J. Virol. 69:513–516.
27. Sakata H, Hishiyama M, Sugiura A. 1984. Enzyme-linked immunosorbent assay compared with neutralization tests for evaluation of live mumps vaccines. J. Clin. Microbiol. 19:21–25.
28. Takeda M, Takeuchi K, Miyajima N, Kobune F, Ami Y, Nagata N, Suzaki Y, Nagai Y, Tashiro M. 2000. Recovery of pathogenic measles virus from cloned cDNA. J. Virol. 74:6643–6647.
29. Radecke F, Spielhofer P, Schneider H, Kaelin K, Huber M, Dotsch C, Christiansen G, Billeter MA. 1995. Rescue of measles viruses from cloned DNA. EMBO J. 14:5773–5784.
30. Hashimoto K, Ono N, Tatsuo H, Minagawa H, Takeda M, Takeuchi K, Yanagi Y. 2002. SLAM (CD150)-independent measles virus entry as revealed by recombinant virus expressing green fluorescent protein. J. Virol. 76:6743–6749.
31. Tahara M, Takeda M, Seki F, Hashiguchi T, Yanagi Y. 2007. Multiple amino acid substitutions in hemagglutinin are necessary for wild-type measles virus to acquire the ability to use receptor CD46 efficiently. J. Virol. 81:2564–2572.
32. Tahara M, Takeda M, Shirogane Y, Hashiguchi T, Ohno S, Yanagi Y. 2008. Measles virus infects both polarized epithelial and immune cells by using distinctive receptor-binding sites on its hemagglutinin. J. Virol. 82:4630–4637.
33. Seki F, Yamada K, Nakatsu Y, Okamura K, Yanagi Y, Nakayama T, Komase K, Takeda M. 2011. The SI strain of measles virus derived from a patient with subacute sclerosing panencephalitis possesses typical genome alterations and unique amino acid changes that modulate receptor specificity and reduce membrane fusion activity. J. Virol. 85:11871–11882.

34. Brindley MA, Plemper RK. 2010. Blue native PAGE and biomolecular complementation reveal a tetrameric or higher-order oligomer organization of the physiological measles virus attachment protein H. J. Virol. 84:12174–12184.
35. Plemper RK, Hammond AL, Gerlier D, Fielding AK, Cattaneo R. 2002. Strength of envelope protein interaction modulates cytopathicity of measles virus. J. Virol. 76:5051–5061.
36. Paal T, Brindley MA, St Clair C, Prussia A, Gaus D, Krumm SA, Snyder JP, Plemper RK. 2009. Probing the spatial organization of measles virus fusion complexes. J. Virol. 83:10480–10493.
37. Corey EA, Iorio RM. 2009. Measles virus attachment proteins with impaired ability to bind CD46 interact more efficiently with the homologous fusion protein. Virology 383:1–5.
38. Tahara M, Takeda M, Yanagi Y. 2005. Contributions of matrix and large protein genes of the measles virus Edmonston strain to growth in cultured cells as revealed by recombinant viruses. J. Virol. 79:15218–15225.
39. Takeda M, Ohno S, Tahara M, Takeuchi H, Shirogane Y, Ohmura H, Nakamura T, Yanagi Y. 2008. Measles viruses possessing the polymerase protein genes of the Edmonston vaccine strain exhibit attenuated gene expression and growth in cultured cells and SLAM knock-in mice. J. Virol. 82:11979–11984.
40. Leonard VH, Sinn PL, Hodge G, Miest T, Devaux P, Oezguen N, Braun W, McCray PB, McChesney MB, Cattaneo R. 2008. Measles virus blind to its epithelial cell receptor remains virulent in rhesus monkeys but cannot cross the airway epithelium and is not shed. J. Clin. Invest. 118:2448–2458.
41. Ertl OT, Wenz DC, Bouche FB, Berbers GA, Muller CP. 2003. Immunodominant domains of the Measles virus hemagglutinin protein eliciting a neutralizing human B cell response. Arch. Virol. 148:2195–2206.
42. Hu A, Sheshberadaran H, Norrby E, Kovamees J. 1993. Molecular characterization of epitopes on the measles virus hemagglutinin protein. Virology 192:351–354.
43. Rota JS, Hummel KB, Rota PA, Bellini WJ. 1992. Genetic variability of the glycoprotein genes of current wild-type measles isolates. Virology 188: 135–142.
44. Sakata H, Kobune F, Sato TA, Tanabayashi K, Yamada A, Sugiura A. 1993. Variation in field isolates of measles virus during an 8-year period in Japan. Microbiol. Immunol. 37:233–237.
45. Patterson JB, Scheiflinger F, Manchester M, Yilma T, Oldstone MB. 1999. Structural and functional studies of the measles virus hemagglutinin: identification of a novel site required for CD46 interaction. Virology 256:142–151.
46. Rota PA, Brown K, Mankertz A, Santibanez S, Shulga S, Muller CP, Hubschen JM, Siqueira M, Beirnes J, Ahmed H, Triki H, Al-Busaidy S, Dosseh A, Byabamazima C, Smit S, Akoua-Koffi C, Bwogi J, Bukenya H, Wairagkar N, Ramamurty N, Incomserb P, Pattamadilok S, Jee Y, Lim W, Xu W, Komase K, Takeda M, Tran T, Castillo-Solorzano C, Chenoweth P, Brown D, Mulders MN, Bellini WJ, Featherstone D. 2011. Global distribution of measles genotypes and measles molecular epidemiology. J. Infect. Dis. 204(Suppl 1):S514–S523.
47. Fournier P, Brons NH, Berbers GA, Wiesmuller KH, Fleckenstein BT, Schneider F, Jung G, Muller CP. 1997. Antibodies to a new linear site at the topographical or functional interface between the haemagglutinin and fusion proteins protect against measles encephalitis. J. Gen. Virol. 78(Pt 6):1295–1302.
48. Duke T, Mgone CS. 2003. Measles: not just another viral exanthem. Lancet 361:763–773.
49. Ader N, Brindley MA, Avila M, Origgi FC, Langedijk JP, Orvell C, Vandevelde M, Zurbriggen A, Plemper RK, Plattet P. 2012. Structural rearrangements of the central region of the morbillivirus attachment protein stalk domain trigger F protein refolding for membrane fusion. J. Biol. Chem. 287:16324–16334.
50. Makela MJ, Salmi AA, Norrby E, Wild TF. 1989. Monoclonal antibodies against measles virus haemagglutinin react with synthetic peptides. Scand. J. Immunol. 30:225–231.
51. Ziegler D, Fournier P, Berbers GA, Steuer H, Wiesmuller KH, Fleckenstein B, Schneider F, Jung G, King CC, Muller CP. 1996. Protection against measles virus encephalitis by monoclonal antibodies binding to a cystine loop domain of the H protein mimicked by peptides which are not recognized by maternal antibodies. J. Gen. Virol. 77(Pt 10):2479–2489.
52. Putz MM, Hoebeke J, Ammerlaan W, Schneider S, Muller CP. 2003. Functional fine-mapping and molecular modeling of a conserved loop epitope of the measles virus hemagglutinin protein. Eur. J. Biochem. 270: 1515–1527.
53. Liebert UG, Flanagan SG, Loffler S, Baczko K, ter Meulen V, Rima BK. 1994. Antigenic determinants of measles virus hemagglutinin associated with neurovirulence. J. Virol. 68:1486–1493.

JVI
Journals.ASM.org

The Receptor-Binding Site of the Measles Virus Hemagglutinin Protein Itself Constitutes a Conserved Neutralizing Epitope

Maino Tahara,[a] Shinji Ohno,[b] Kouji Sakai,[a] Yuri Ito,[c] Hideo Fukuhara,[c] Katsuhiro Komase,[a] Melinda A. Brindley,[d] Paul A. Rota,[e] Richard K. Plemper,[d] Katsumi Maenaka,[c] Makoto Takeda[a]

Department of Virology 3, National Institute of Infectious Diseases, Tokyo, Japan[a]; Department of Virology, Faculty of Medicine, Kyushu University, Fukuoka, Japan[b]; Laboratory of Biomolecular Science, Faculty of Pharmaceutical Sciences, Hokkaido University, Hokkaido, Japan[c]; Department of Pediatrics, Emory University School of Medicine, Atlanta, Georgia, USA[d]; Measles, Mumps, Rubella and Herpesviruses Laboratory Branch, Division of Viral Diseases, Centers for Disease Control and Prevention, Atlanta, Georgia, USA[e]

Here, we provide direct evidence that the receptor-binding site of measles virus (MV) hemagglutinin protein itself forms an effective conserved neutralizing epitope (CNE). Several receptor-interacting residues constitute the CNE. Thus, viral escape from neutralization has to be associated with loss of receptor-binding activity. Since interactions with both the signaling lymphocyte activation molecule (SLAM) and nectin4 are critical for MV pathogenesis, its escape, which results from loss of receptor-binding activity, should not occur in nature.

Measles virus (MV) is an enveloped virus that belongs to the genus *Morbillivirus* of the family *Paramyxoviridae* and possesses two types of surface glycoprotein spikes, the hemagglutinin (H) and fusion (F) proteins. MV infection is initiated by binding of the H protein to cellular receptors on the target host cells. The binding triggers membrane fusion between the virus envelope and the host cell plasma membrane mediated by the F protein. The signaling lymphocyte activation molecule (SLAM) on a subset of immune cells and nectin4 at adherens junctions are the principal receptors for MV (1–4). The H and F proteins are both neutralizing targets, but greater amounts of antibodies (Abs) are elicited against the H protein than the F protein, and the H protein-specific antibodies mainly contribute to neutralization of MV infection *in vivo* (5–8). All the available data suggest that measles eradication is biologically feasible (9, 10), and one of the major factors that would ensure measles eradication is the single-serotype nature of MV. Our previous paper suggested that the receptor-binding site (RBS) on the H protein, which is exposed outside the heavy N-glycan shields, may constitute a major neutralizing epitope that contributes to the single-serotype nature of MV (11). However, our recent paper (12) showing the detailed locations of five epitopes (*I*, *II*, *iv*, *v*, and *vi*) on the H protein provided insufficient evidence that the RBS acts as a neutralizing epitope. Here, we provide direct and concrete evidence that the RBS itself forms an effective conserved neutralizing epitope (CNE) which provides a strong functional constraint against change.

In the present study, we characterized a new mouse monoclonal antibody (MAb), 2F4. MAb 2F4 was produced using a cell line expressing the H protein of the wild-type IC-B strain as an antigen. For competitive binding enzyme-linked immunosorbent assays (cELISAs), MV antigens precoated on cELISA plates (Denka Seiken) were incubated with previously reported MAbs (E81, E128, E185, E39, and E103) (12, 13), 2F4, or phosphate-buffered saline for 1 h and then incubated with MAb 2F4 labeled with biotin using a biotin labeling kit (NH2; Dojindo Laboratories). After three washes, the MV antigens bound by the MAbs were incubated with a streptavidin-horseradish peroxidase (HRP) conjugate (Thermo Scientific) for 1 h before addition of the TMB substrate (3,3′5,5′-tetramethylbenzidine; Denka Seiken). The plates were incubated for 25 min, and the colorimetric reactions were stopped by addition of H_2SO_4. The optical density (OD) values were analyzed using a microplate reader (Bio-Rad). The data revealed that binding of 2F4 was not inhibited by MAbs recognizing epitopes *I*, *iv*, *v*, and *vi* (E81, E185, E39, and E103, respectively) (12) (Table 1; the epitope recognized by 2F4 is tentatively termed epitope *vii*). On the other hand, E128 recognizing epitope *II* (12) showed partial inhibition of 2F4 binding (Table 1). Epitope *II* is shielded by the N-glycan modification at amino acid position 416 (N416-sugar), and viruses with the N416-sugar (genotypes D3, D4, D5, and D9 among the eight genotypes) are not neutralized by E128 (12). Eight distinct recombinant MVs (rMVs) encoding a *Renilla* luciferase reporter gene and an H gene derived from different MV genotypes (A, B3, D3, D4, D5, D8, D9, and H1) were used as neutralization targets for 2F4 (Table 2), as reported previously (12). The data clearly demonstrated that, unlike E128 recognizing epitope *II*, 2F4 showed high neutralizing titers against all eight rMVs (Table 2). These data suggested that epitope *vii* is a CNE and is distinct from all the other five epitopes (*I*, *II*, *iv*, *v*, and *vi*).

When the H protein-SLAM interaction was assessed by surface plasmon resonance assays, as reported previously (12), MAb 2F4 blocked binding of the H protein to SLAM, as did MAbs B5 and E128 recognizing epitopes *I* and *II*, which are located near the RBS (12) (Table 3). These data suggest that epitope *vii* is located at or near the RBS. A panel of rMVs possessing amino acid substitutions at the RBS were analyzed for neutralization by 2F4. On the D3 genetic background (IC323 strain [14]), four rMVs encoding enhanced green fluorescent protein (EGFP) and possessing mutations at a SLAM-interacting residue (R533A) (Fig. 1B) and nectin4-interacting residues (F483A, Y543S, and S544A/Y541S) (Fig.

Received 29 October 2012 **Accepted** 26 December 2012
Published ahead of print 2 January 2013
Address correspondence to Maino Tahara, maino@nih.go.jp.

doi:10.1128/JVI.03029-12

TABLE 1 Summary of competitive binding ELISAs of anti-H protein MAbs

Unlabeled MAb	Antigenic site	Biotinylated MAb 2F4 (*vii*) inhibition[a]
E81	*I*	−
E128	*II*	+
E185	*iv*	−
E39	*v*	−
E103	*vi*	−
2F4	*vii*	++

[a] ++, complete inhibition; +, partial inhibition; −, no inhibition.

1C) (15–19) were generated and assessed for virus spreading in SLAM-positive (SLAM$^+$) B95a and nectin4$^+$ II-18 cells (20) in the presence or absence of 2F4 (Fig. 2). The rMVs with F483A and Y543S were reported previously (15). As shown in Fig. 2, in the absence of 2F4 [Ab(−)], wild-type MV spread efficiently in both cell types using SLAM or nectin4. On the other hand, rMVs with F483A, Y543S, or S544A/Y541S lost the ability to use nectin4 as a receptor and thus failed to spread in II-18 cells, even in the absence of 2F4. Similarly, rMV with R533A lost the ability to use SLAM as a receptor and did not spread in B95a cells. However, in the presence of 2F4, the mutant MVs showed advantages for spreading. Even in the presence of 2F4, rMVs with F483A, Y543S, or S544A/Y541S were able to spread in SLAM$^+$ B95a cells, and rMV with R533 was able to spread in nectin4$^+$ II-18 cells, whereas the wild-type MV infection was completely neutralized by 2F4. Similar experiments were performed using luciferase-expressing rMVs (21). Two rMVs with mutations at SLAM-interacting residues (D505S and R533A) (17, 19) (Fig. 1B) and two rMVs with mutations at nectin4-interacting residues (F483A and Y543S) (15, 16, 18) (Fig. 1C) were generated (rMVs with F483A and Y543S were reported previously [15]). In part, as reported previously, rMVs with F483A (15) and Y543S (15) were unable to bind to nectin4 (2, 3), and those with R533A (16) and D505S (in the present study) lost the ability to use SLAM (Table 4). Meanwhile, the F483A, Y543S, D505S, and R533A substitutions all resulted in escape from neutralization by 2F4 (Table 4). These data demonstrated that the RBS used for interactions with both SLAM and nectin4 constitutes epitope *vii* recognized by 2F4 (Fig. 1). Consequently, MV escape

TABLE 2 Neutralizing titers against MV strains possessing H genes from different genotypes

Cell line	Genotype, yr isolated	Neutralizing titer[a] 2F4 (*vii*)	Neutralizing titer[a] E128 (*II*)[b]
B95a	A, 1954	22,141	1,968
	B3, 2009	11,070	1,968
	D3, 1984	22,141	15
	D4, 2009	22,141	31
	D5, 2001	11,070	15
	D8, 2009	44,281	1,968
	D9, 2010	11,070	15
	H1, 2009	22,141	1,968
II-18	A, 1954	11,070	62,977
	B3, 2009	11,070	62,977
	D3, 1984	11,070	123
	D4, 2009	11,070	31
	D5, 2001	22,141	<4
	D8, 2009	22,141	62,977
	D9, 2010	11,070	123
	H1, 2009	22,141	62,977

[a] Data represent neutralizing titers for 1 mg/ml of immunoglobulin.
[b] Data for E128 are taken from reference 12.

TABLE 3 Competitive binding of anti-H protein MAbs against SLAM[a]

MAb	Antigenic site	Competitive activity[b]
2F4	*vii*	++
B5	*I*	++
E128	*II*	++
E103	*vi*	−

[a] The detailed procedure has been previously reported (12).
[b] ++, complete inhibition; −, no inhibition.

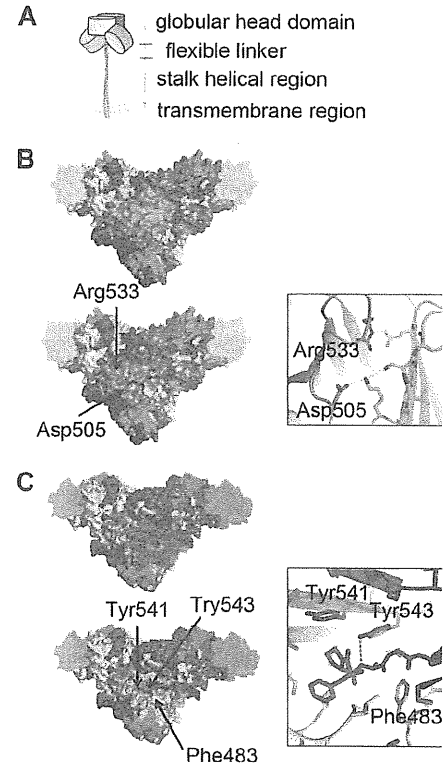

FIG 1 Location of epitope *vii* on the H protein tetrameric structure. (A) Diagram of an H protein tetramer (a dimer of H protein dimers). The four H protein molecules are shown in dark gray, light gray, dark purple, and light purple. (B) Location of SLAM-interacting residues, which constitute epitope *vii* on the tetrameric H protein structure in complex with SLAM (19). SLAM is shown in translucent cyan. SLAM interacting with the gray H protein is deleted in the structure shown at the bottom. A detailed view in a ribbon and stick diagram is shown in the box. SLAM is shown in cyan, and H protein is shown in orange or yellow. (C) Location of nectin4-interacting residues, which constitute epitope *vii*. The tetrameric structure was reconstructed using data by Hashiguchi et al. (19) and Zhang et al. (18). Nectin4 is shown in translucent magenta. Nectin4 interacting with the gray H protein is deleted in the structure shown at the bottom. A detailed view in a ribbon and stick diagram is shown in the box. Nectin4 is shown in magenta, and H protein is shown in orange or yellow. (B and C) The figures were produced using PyMOL (Schrödinger; http://www.pymol.org). The amino acid residues demonstrated or suggested to constitute portions of epitopes are shown in colors as follows: residues on beta-sheets 1, 2, 3, 4, 5, and 6 (19) are shown in blue, dark green, light green, yellow, orange, and red, respectively.

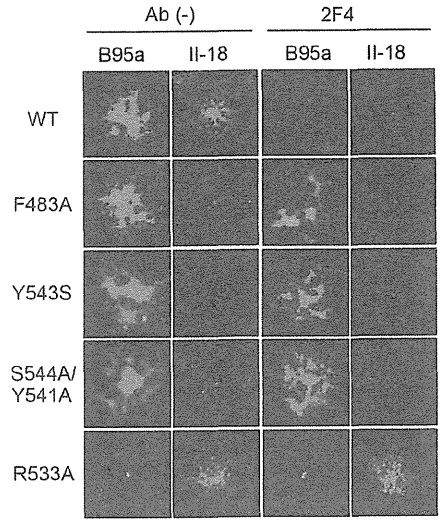

FIG 2 Effects of specific substitutions on virus infectivity and MAb neutralization. EGFP autofluorescence in MV-infected SLAM$^+$ B95a cells and nectin4$^+$ II-18 cells is shown. B95a and II-18 cells were infected with rMVs containing F483A, Y543S, S544A/Y541S, and R533A substitutions in the presence or absence of MAb 2F4. The panels show representative images observed using a fluorescence microscope.

from neutralization by 2F4 is penalized by loss of affinity for one of the principal MV receptors.

Apparently, a previously reported MAb, I-41, also recognizes this *vii* epitope (22), since a substitution at position 552 (the phenylalanine at this position is predicted to interact with SLAM [19]) allowed MV to escape from neutralization. Another previous study implied that MAb 80-II-B2 recognizes a region containing residues 505 and 506 within this epitope (23). The H protein of the CAM-70 MV vaccine strain features a mutation at position 505. Accordingly, the CAM-70 vaccine strain does not react with 80-II-B2 and binds to SLAM inefficiently (23, 24). Previous competitive binding studies revealed that MAb 16-DE6 recognizes the same antigenic site as I-41 (25), and that an 16-DE6 escape mutant contained, among other changes, an arginine-to-glycine substitution at position 533 (R533G) (22). Previously characterized MAbs B2 and BH26 similarly recognize this epitope (6, 25, 26), which appears to be a premier neutralizing epitope for the H protein. Residues located in this epitope may be involved in SLAM-binding activity (6, 26). Therefore, this region probably corresponds to epitope *vii* identified in our study.

In summary, the present data demonstrate that both the SLAM- and nectin4-interacting residues themselves constitute a CNE. Since these residues are critical for interaction with either SLAM or nectin4, viral escape from neutralization has to be associated with loss of the receptor-binding activity. Since efficient MV spreading mandates interactions of the H protein with these two discrete proteinaceous receptors, SLAM and nectin4 (4), residues within this domain are likely to be under high selective pressure to maintain their molecular identity, and contribute to the sustainability of the single-serotype nature of MV.

TABLE 4 Neutralizing titers against recombinant MVs possessing the IC-H protein with various amino acid substitutions

Cell line	Mutation	Infectivity	Neutralizing titer[a]			
			B5 (*I*)	E81 (*I*)	E103 (*vi*)	2F4 (*vii*)
B95a	Wild type (−)	+	7,536	1,727	10,231	22,141
	F483A	+	3,768	1,727	10,231	<346
	Y543S	+	1,884	1,727	2,558	692
	D505S	−	NA	NA	NA	NA
	R533A	−	NA	NA	NA	NA
II-18	Wild type (−)	+	3,764	27,631	20,462	11,070
	F483A	−	NA	NA	NA	NA
	Y543A	−	NA	NA	NA	NA
	D505S	+	1,884	13,815	20,462	<5
	R533A	+	1,884	27,631	20,462	173

[a] Data represent neutralizing titers for 1 mg/ml of immunoglobulin. NA, not applicable.

ACKNOWLEDGMENTS

We thank T.A. Sato, Y. Yanagi, and T. Seya for providing MAbs, N. Ito and M. Sugiyama for providing BHK/T7-9 cells, and K. Taira for providing an MV isolate. We also thank all the members of Department of Virology 3, NIID, Japan, for technical support.

REFERENCES

1. Tatsuo H, Ono N, Tanaka K, Yanagi Y. 2000. SLAM (CDw150) is a cellular receptor for measles virus. Nature 406:893–897.
2. Noyce RS, Bondre DG, Ha MN, Lin LT, Sisson G, Tsao MS, Richardson CD. 2011. Tumor cell marker PVRL4 (nectin 4) is an epithelial cell receptor for measles virus. PLoS Pathog. 7:e1002240. doi:10.1371/journal.ppat.1002240.
3. Mühlebach MD, Mateo M, Sinn PL, Prufer S, Uhlig KM, Leonard VH, Navaratnarajah CK, Frenzke M, Wong XX, Sawatsky B, Ramachandran S, McCray PB, Jr, Cichutek K, von Messling V, Lopez M, Cattaneo R. 2011. Adherens junction protein nectin-4 is the epithelial receptor for measles virus. Nature 480:530–533.
4. Takeda M, Tahara M, Nagata N, Seki F. 2011. Wild-type measles virus is intrinsically dual-tropic. Front. Microbiol. 2:279. doi:10.3389/fmicb.2011.00279.
5. de Swart RL, Yuksel S, Osterhaus AD. 2005. Relative contributions of measles virus hemagglutinin- and fusion protein-specific serum antibodies to virus neutralization. J. Virol. 79:11547–11551.
6. Bouche FB, Ertl OT, Muller CP. 2002. Neutralizing B cell response in measles. Viral Immunol. 15:451–471.
7. de Swart RL, Yuksel S, Langerijs CN, Muller CP, Osterhaus AD. 2009. Depletion of measles virus glycoprotein-specific antibodies from human sera reveals genotype-specific neutralizing antibodies. J. Gen. Virol. 90:2982–2989.
8. Duke T, Mgone CS. 2003. Measles: not just another viral exanthem. Lancet 361:763–773.
9. Sanders R, Dabbagh A, Featherstone D. 2011. Risk analysis for measles reintroduction after global certification of eradication. J. Infect. Dis. 204(Suppl 1):S71–S77.
10. Bellini WJ, Rota PA. 2011. Biological feasibility of measles eradication. Virus Res. 162:72–79.
11. Hashiguchi T, Kajikawa M, Maita N, Takeda M, Kuroki K, Sasaki K, Kohda D, Yanagi Y, Maenaka K. 2007. Crystal structure of measles virus hemagglutinin provides insight into effective vaccines. Proc. Natl. Acad. Sci. U. S. A. 104:19535–19540.
12. Tahara M, Ito Y, Brindley MA, Ma X, He J, Xu S, Fukuhara H, Sakai K, Komase K, Rota PA, Plemper RK, Maenaka K, Takeda M. 2013. Functional and structural characterization of neutralizing epitopes of measles virus hemagglutinin protein. J. Virol. 87:666–675.
13. Sato TA, Fukuda A, Sugiura A. 1985. Characterization of major structural proteins of measles virus with monoclonal antibodies. J. Gen. Virol. 66(Pt 7):1397–1409.
14. Takeda M, Takeuchi K, Miyajima N, Kobune F, Ami Y, Nagata N, Suzaki Y, Nagai Y, Tashiro M. 2000. Recovery of pathogenic measles virus from cloned cDNA. J. Virol. 74:6643–6647.
15. Tahara M, Takeda M, Shirogane Y, Hashiguchi T, Ohno S, Yanagi Y.

2008. Measles virus infects both polarized epithelial and immune cells by using distinctive receptor-binding sites on its hemagglutinin. J. Virol. 82: 4630–4637.
16. Leonard VH, Sinn PL, Hodge G, Miest T, Devaux P, Oezguen N, Braun W, McCray PB, McChesney MB, Cattaneo R. 2008. Measles virus blind to its epithelial cell receptor remains virulent in rhesus monkeys but cannot cross the airway epithelium and is not shed. J. Clin. Invest. 118:2448–2458.
17. Vongpunsawad S, Oezgun N, Braun W, Cattaneo R. 2004. Selectively receptor-blind measles viruses: identification of residues necessary for SLAM- or CD46-induced fusion and their localization on a new hemagglutinin structural model. J. Virol. 78:302–313.
18. Zhang X, Lu G, Qi J, Li Y, He Y, Xu X, Shi J, Zhang C, Yan J, Gao GF. 2013. Structure of measles virus hemagglutinin bound to its epithelial receptor nectin-4. Nat. Struct. Mol. Biol. 20:67–72.
19. Hashiguchi T, Ose T, Kubota M, Maita N, Kamishikiryo J, Maenaka K, Yanagi Y. 2011. Structure of the measles virus hemagglutinin bound to its cellular receptor SLAM. Nat. Struct. Mol. Biol. 18:135–141.
20. Shirogane Y, Takeda M, Tahara M, Ikegame S, Nakamura T, Yanagi Y. 2010. Epithelial-mesenchymal transition abolishes the susceptibility of polarized epithelial cell lines to measles virus. J. Biol. Chem. 285:20882–20890.
21. Takeda M, Ohno S, Tahara M, Takeuchi H, Shirogane Y, Ohmura H, Nakamura T, Yanagi Y. 2008. Measles viruses possessing the polymerase protein genes of the Edmonston vaccine strain exhibit attenuated gene expression and growth in cultured cells and SLAM knock-in mice. J. Virol. 82:11979–11984.
22. Hu A, Sheshberadaran H, Norrby E, Kovamees J. 1993. Molecular characterization of epitopes on the measles virus hemagglutinin protein. Virology 192:351–354.
23. Hummel KB, Bellini WJ. 1995. Localization of monoclonal antibody epitopes and functional domains in the hemagglutinin protein of measles virus. J. Virol. 69:1913–1916.
24. Kato S, Ohgimoto S, Sharma LB, Kurazono S, Ayata M, Komase K, Takeda M, Takeuchi K, Ihara T, Ogura H. 2009. Reduced ability of hemagglutinin of the CAM-70 measles virus vaccine strain to use receptors CD46 and SLAM. Vaccine 27:3838–3848.
25. Sheshberadaran H, Norrby E. 1986. Characterization of epitopes on the measles virus hemagglutinin. Virology 152:58–65.
26. Ertl OT, Wenz DC, Bouche FB, Berbers GA, Muller CP. 2003. Immunodominant domains of the Measles virus hemagglutinin protein eliciting a neutralizing human B cell response. Arch. Virol. 148:2195–2206.

zjv00813/zjv7521d13z | xppws | S=1 | 2/18/13 | 4:46 | 4/C Fig: 1,2,3,4,5,6 | Facing: 6-7 | ArtID: 02189-12 | NLM: research-article | CE: pmw

Editor: Garcia-Sastre | Section: Virus-Cell Interactions | Designation: T

JVI Journals.ASM.org

Intracellular Transport of the Measles Virus Ribonucleoprotein Complex Is Mediated by Rab11A-Positive Recycling Endosomes and Drives Virus Release from the Apical Membrane of Polarized Epithelial Cells

AQ: au

Yuichiro Nakatsu,[a] Xuemin Ma,[a] Fumio Seki,[a] Tadaki Suzuki,[b] Masaharu Iwasaki,[c] Yusuke Yanagi,[c] Katsuhiro Komase,[a] Makoto Takeda[a]

Department of Virology 3, National Institute of Infectious Diseases, Tokyo, Japan[a]; Department of Pathology, National Institute of Infectious Diseases, Tokyo, Japan[b]; Department of Virology, Faculty of Medicine, Kyushu University, Fukuoka, Japan[c]

Many viruses use the host trafficking system at a variety of their replication steps. Measles virus (MV) possesses a nonsegmented negative-strand RNA genome that encodes three components of the ribonucleoprotein (RNP) complex (N, P, and L), two surface glycoproteins, a matrix protein, and two nonstructural proteins. A subset of immune cells and polarized epithelial cells are *in vivo* targets of MV, and MV is selectively released from the apical membrane of polarized epithelial cells. However, the molecular mechanisms for the apical release of MV remain largely unknown. In the present study, the localization and trafficking mechanisms of the RNP complex of MV were analyzed in detail using recombinant MVs expressing fluorescent protein-tagged L proteins. Live cell imaging analyses demonstrated that the MV RNP complex was transported in a manner dependent on the microtubule network and together with Rab11A-containing recycling endosomes. The RNP complex was accumulated at the apical membrane and the apical recycling compartment. The accumulation and shedding of infectious virions were severely impaired by expression of a dominant negative form of Rab11A. On the other hand, recycling endosome-mediated RNP transport was totally dispensable for virus production in nonpolarized cells. These data provide the first demonstration of the regulated intracellular trafficking events of the MV RNP complex that define the directional viral release from polarized epithelial cells.

AQ: A

For airborne viruses, efficient shedding of progeny viruses is critical for transmission. Measles virus (MV) is the causative agent of measles, which is an acute and highly contagious disease characterized by high fever and a maculopapular rash. MV is an enveloped virus that belongs to the genus *Morbillivirus* in the family *Paramyxoviridae*. The MV genome is a nonsegmented negative-sense RNA encoding six tandemly linked genes, N, P/V/C, M, F, H, and L (1). Each virion contains the RNA genome encapsidated by the nucleocapsid (N) protein. The encapsidated genome is associated with a viral RNA-dependent RNA polymerase composed of the phospho- (P) and large (L) proteins and forms the ribonucleoprotein (RNP) complex. The virus particle possesses two types of glycoprotein spikes, the hemagglutinin (H) and fusion (F) proteins, on the envelope. The H protein is responsible for binding to cellular receptors, while the F protein mediates membrane fusion between the virus envelope and the host cell plasma membrane. The matrix (M) protein is also a major component of the virus particle and plays crucial roles in virus assembly by associating with the cytoplasmic tails of the F and H proteins as well as the RNP complex. In addition to these structural components, the MV genome encodes two nonstructural proteins, V and C, which are synthesized in infected cells and counteract host interferon responses. Recent studies showed that polarized epithelial cells are infected with MV via nectin4 as a receptor, a process that is critical for virus shedding *in vivo* (2–4). Progeny MV particles are selectively released from the apical plasma membrane of polarized epithelial cells (5, 6). It is well known that MV replicates entirely within the cytoplasm, but the detailed location for each event, such as viral RNA synthesis, is poorly elucidated. Moreover, little is known about the molecular mechanisms underlying the directional virus release from polarized epithelial cells. Previous studies demonstrated that the viral RNP complexes of influenza A virus (IAV) in the family *Orthomyxoviridae* and Sendai virus (SeV) in the family *Paramyxoviridae* are transported along microtubules (MTs) using Rab11-positive recycling endosomes (REs) (7–10). The Rab11 GTPase subfamily consists of Rab11a, Rab11b, and Rab25/Rab11c, which play key roles in protein traffic by REs. Similarly, vesicular stomatitis virus (VSV) in the family *Rhabdoviridae* also uses MTs for its protein transport (11). In the present study, the intracellular location and trafficking of the RNP complex of MV were analyzed.

MATERIALS AND METHODS

Plasmids. The full-length genome plasmid p(+)MV323-EGFPtagL encoding the MV genome with an enhanced green fluorescent protein (EGFP)-tagged L gene was described previously (12, 13). The full-length genome plasmid p(+)MV323-mCherrytagL was generated by replacing the EGFP cDNA region of p(+)MV323-EGFPtagL with an mCherry cDNA. The full-length genome plasmid p(+)MV323-AddmCherry was generated by introducing the mCherry gene into an additional transcriptional unit between the H and L genes, as reported previously (14).

Received 16 August 2012 Accepted 5 February 2013

Published ahead of print 13 February 2013

Address correspondence to Yuichiro Nakatsu, ynakatsu@nih.go.jp.

Supplemental material for this article may be found at http://dx.doi.org/10.1128/JVI.02189-12.

doi:10.1128/JVI.02189-12

pTagRFP-Tubulin and pAcGFP1-Tubulin were purchased from Evrogen (Moscow, Russia) and Clontech (Mountain View, CA), respectively. These plasmids encode red fluorescent protein (RFP)- and green fluorescent protein (GFP)-tagged α-tubulin, which are reported to behave similarly to untagged α-tubulin (10, 15, 16). The expression plasmids pMXsIP-EGFP, pMXsIP-EGFP-Rab5, pMXsIP-EGFP-Rab7, and pMXsIP-EGFP-Rab11A and the EGFP-tagged dominant negative form of Rab11A (Rab11A-S25N) (pMXsIP-EGFP-Rab11ADN) were generated by inserting the cDNAs of the respective Rab genes with N-terminally fused EGFP into the multicloning site of pMXsIP (17). A retroviral vector encoding a short-hairpin RNA (shRNA) against Rab11A mRNA (pSUPER-retro-shRab11A) was constructed by inserting the oligonucleotide fragment (target sequence, 5′-AAGAGCACCATTGGAGTAGAG-3′) into pSUPER.retro.puro (Oligoengine, Seattle, WA). As a negative control, a retroviral vector with an oligonucleotide fragment (target sequence, 5′-AAGCGCGCTTTGTAGGATTCG-3′) (pSUPERretro-shNC) was also prepared. Retroviral preparations were performed according to the manufacturer's instructions.

AQ: B

Cells and virus. Vero/hSLAM cells (18), BHK/T7-9 cells (kindly provided by N. Ito) (19), and MDCK II cells were maintained in Dulbecco's modified Eagle's medium (DMEM) (Sigma, St. Louis, MO) containing 7% fetal bovine serum (FBS). PLAT-gp cells, a 293T-derived Moloney murine leukemia virus (MMLV)-based retroviral vector packaging cell line (kindly provided by M. Shimojima and T. Kitamura) (20), were maintained in DMEM containing 10% FBS. MMLV-based retroviral vectors expressing EGFP or EGFP-tagged Rab proteins were produced by introducing the corresponding pMXsIP vector (pMXsIP-EGFP, -EGFP-Rab5, -EGFP-Rab7, -EGFP-Rab11A, or -EGFP-Rab11ADN) together with a VSV G protein-expressing plasmid, pCVSV-G, into PLAT-gp cells (17). Vero/hSLAM or MDCK cells constitutively expressing EGFP, EGFP-Rab5, EGFP-Rab7, EGFP-Rab11A, or EGFP-Rab11ADN were then generated by transduction of the respective genes using the MMLV-based retroviral vector and selection with puromycin (17). Vero/hSLAM cells constitutively expressing negative-control shRNA (Vero/hSLAM/shNC) or shRNA against Rab11A (Vero/hSLAM/shRab11A) were generated by transduction of the respective shRNA using the retroviral vector and selection with puromycin. IC323 (21) and IC323-EGFPtagL (13) were reported previously. IC323-mCherrytagL and IC323-AddmCherry were generated from p(+)MV323-mCherrytagL and p(+)MV323-AddmCherry, respectively, using an efficient MV reverse genetics system (22). All of the recombinant MVs (rMVs) used in this study were propagated in Vero/hSLAM cells, and the infectious virus titers were determined by plaque assays.

Growth kinetics analysis of MV. Vero/hSLAM cells were infected with MV at a multiplicity of infection (MOI) of 0.01. At various time points, the culture medium or the cells were harvested and the infectious virus titers (in plaque-forming units [PFU]) were determined by standard plaque assays on Vero/hSLAM cells. MDCK cells on 24-well plates or 12-mm filter units of tissue culture-treated 0.4-μm-pore-size transwell polycarbonate filters (Costar Corp., Cambridge, MA) were infected with MV at an MOI of 0.2 immediately after cell seeding, since confluent monolayers of MDCK cells are poorly susceptible to MV infection (6). The formation of an electrically tight monolayer was checked daily by measuring the transepithelial resistance using an ERS-2 apparatus (Millipore, Bedford, MA). At various time points, the culture medium or the cells were harvested and the infectious virus titers were determined by plaque assays on Vero/hSLAM cells.

Reagents and antibodies. Nocodazole and paclitaxel were purchased from Sigma. A fusion-blocking peptide (FBP) (Z-D-Phe-Phe-Gly) was purchased from Peptide Institute Inc. (Osaka, Japan). Mouse monoclonal antibodies (MAbs) against the N, C, M, F, and H proteins of MV and a rabbit polyclonal antibody raised against the common N terminus of the P and V proteins were described previously (23, 24). Mouse MAbs against α- and γ-tubulin were purchased from Invitrogen (Carlsbad, CA) and Sigma, respectively. Mouse MAbs raised against EGFP was purchased from Clontech. Rabbit MAbs against Rab11 was purchased from Cell Signaling Technology (Danvers, MA). Alexa Fluor 405-, 488-, 594-, and 647-conjugated anti-mouse and anti-rabbit secondary antibodies were purchased from Invitrogen. 4′,6-Diamidino-2-phenylindole dihydrochloride (DAPI) was purchased from Nacalai Tesque (Kyoto, Japan). Vybrant CM-DiI cell-labeling solution was purchased from Invitrogen and used according to the manufacturer's instructions.

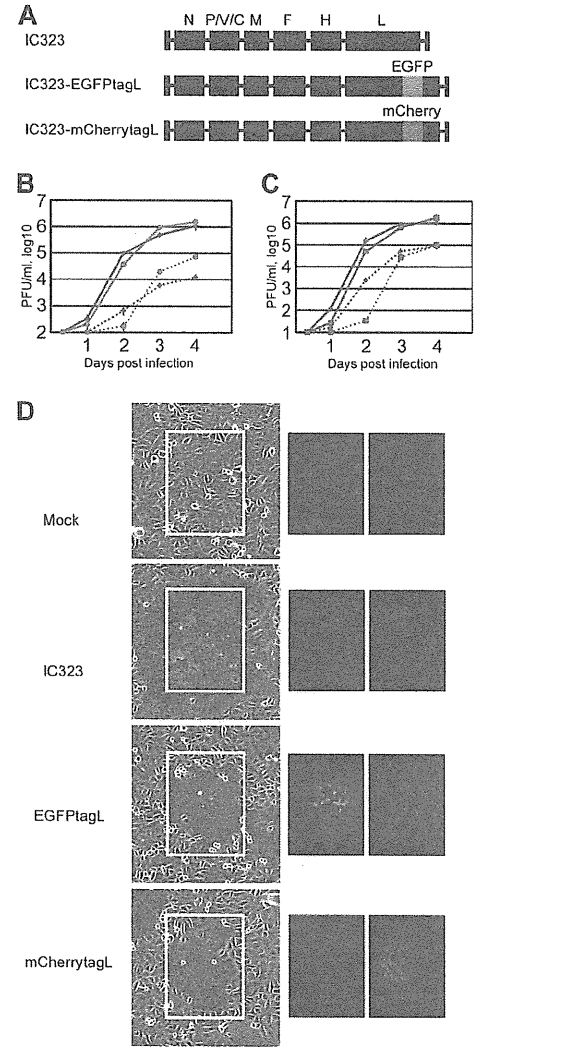

FIG 1 Construction of rMVs expressing FLP-tagged L proteins. (A) Genome structures of the rMVs. The six internal boxes indicate the N, P, M, F, H, and L genes of MV. The portions colored in green and red indicate the coding regions of the green FLP (EGFP) and red FLP (mCherry), respectively. (B and C) Growth kinetics of the rMVs in Vero/hSLAM cells. Vero/hSLAM cells were infected with the rMVs at an MOI of 0.01. At various time points, the cells and culture medium were harvested separately, and the PFU in both samples were determined. The data represent the means ± standard deviations of results from triplicate samples. The solid and dashed lines indicate the data for the cell-associated and cell-free titers, respectively. (B) Blue and green symbols indicate the data for IC323 and IC323-EGFPtagL, respectively. (C) Blue and red symbols indicate the data for IC323 and IC323-mCherrytagL, respectively. (D) Syncytium morphology and FLP-tagged L protein expression in rMV-infected Vero/hSLAM cells. Vero/hSLAM cells were infected with the rMVs at an MOI of 0.01. The cells were observed daily under light and fluorescence microscopes. Data at 2 days p.i. are shown.